Intestinal Regeneration After Irradiation: Stem Cells and Sox9

Brooks Scull

A thesis submitted to the faculty of the University of North Carolina at Chapel Hill in partial fulfillment of the requirements for the degree Master of Science in the Department of Cell and Molecular Physiology.

Chapel Hill
2009

Approved by:

P. Kay Lund

Scott Magness

Michael Helmrath

Abstract

Brooks Scull: Intestinal Regeneration After Irradiation: Stem Cells and Sox9
(Under the direction of P. Kay Lund)

Whole body irradiation is a useful challenge to study the response of intestinal epithelial stem cells (IESC) to genetic damage. High dose irradiation causes complete loss of the proliferative zone within intestinal crypts excluding a few stem/multipotent cells that can regenerate the intestinal epithelial lining. Whole body irradiation models using high dose irradiation are not ideal for studying the regenerative process due to poor animal survival. Little is known about direct effects of irradiation on IESC due to lack of biomarkers. This study developed a high dose abdominal irradiation model with increased survival allowing for analysis of regeneration to day 9 after irradiation and potentially longer. The expression pattern of the putative IESC marker, Sox9, was evaluated and compared with proliferation markers. We provide evidence that differential levels of Sox9 mark subpopulations of proliferating cells. This model will be useful to evaluate therapies that increase IESC survival, proliferation and regeneration.

Acknowledgments

First and foremost, I would like to thank my advisor, Dr. Kay Lund who has been an incredible and irreplaceable mentor. Her scientific knowledge and integity are an inspiration. She started my science career which she continues to nurture and guide for which I am forever in debt.

I would also like to thank the members of my committee, Dr. Michael Helmrath and Dr. Scott Magness for their scientific guidance and advise. They have also been inspirational and integral to my development as a scientist.

I would like to thank my many colleagues and friends in the Cell and Molecular Physiology department. Most notabley, the past and present members of the Lund Lab, especially Jim Simmons, Randy Fuller, Kate Hamilton, Vicki Newton and Nicole Ramocki for their friendship and support.

Finally, I dedicate this thesis to my parents, Chuck and Pat, my brother, Chris, and especially my wife, Jennifer, for their endless love and support throughout the years.

Table of Contents

List of Tables

Table

List of Figures

Figure

Chapter 1

Introduction

Intestinal Physiology

The intestine is a tubular structure consisting of several layers including an outer serosa, longitudinal and circular smooth muscle, the submucosa and an inner mucosa. The mucosa comprises a single layer of epithelial cells facing the lumen, the underlying lamina propria which contains fibroblasts, myofibroblasts, blood vessels and resident immune cells, and the muscularis mucosa. The epithelial lining functions in digestion and absorption of ingested nutrients and as a barrier protecting the underlying tissue from toxins, pathogens and commensal microbiota in the lumen. The epithelial lining of the small intestine is organized into a crypt-villus axis with crypts representing proliferating cells and villi forming finger like projections into the lumen, which provide a larger surface area for digestion and absorption. The colon, like the small intestine has crypts, but does not contain villi {{178 Wright,N.A. 2000}}. In mammals, the epithelium of the small intestine and colon are in a constant state of renewal with turn over of the entire epithelium every 3-10 days depending on the region of the intestine and the species. This renewal is driven by stem or multipotent cells thought to reside at the base of the crypts which maintain the continual process of epithelial renewal. These stem cells are believed to remain at the base of the crypts and continually produce short-lived progenitor or transit amplifying cells that differentiate as they migrate up the

crypt axis and onto the villi or surface epithelium creating a spatially organized hierarchy of cells along the crypt-villus axis . The intestine contains four differentiated cell lineages (Potten & Loeffler, 1990). In the small intestine the lineages include enterocytes, goblet cells, and enteroendercrine cells, which migrate upwards along the crypt-villus axis, while Paneth cells migrate downwards and reside at the very base of the crypts (Figure 1, pg 11). Enterocytes are the most abundant cells in the small intestine and function in absorption and breakdown of nutrients. Goblet cells comprise about 8-10 percent of the cells and secrete mucous that creates a barrier between the epithelium and the luminal contents. Enteroendorcrine cells comprise approximately 4 percent of the intestinal epithelial cells and secrete hormones. There are many types of enteroendocrine cells secreting many different gastrointestinal hormones which regulate gastrointestinal (GI) function (Rindi, Leiter, Kopin, Bordi, & Solcia, 2004). The function of Paneth cells is associated with antimicrobial defense. The average turnover rate of small intestinal epithelial cells in mice is approximately three days, except for Paneth cells which turnover approximately every 50-60 days {{179 Ireland,H. 2005}}. On the luminal surface, a process of cell shedding into the lumen, called anoikis, occurs, which in the healthy intestine is matched by cell renewal in the crypts to maintain constant epithelial mass (Gibson, 2004). These mechanisms of cell proliferation and migration, followed by death and shedding into the lumen are essential to maintain the normal mass, digestive and absorptive functions of the epithelium. In the colon a very similar renewal and differentiation process occurs except normal colon does not contain Paneth cells and cell differentiate as they exit the crypt onto the surface epithelium of the colon.

Intestinal Epithelial Stem Cells

The existence of intestinal epithelial stem/multipotent cells (IESC) at the base of crypts has been recognized for many years, but their exact identity in not fully defined. As early as 1974, proliferating, undifferentiated cells just above and between Paneth cells, referred to as crypt-base columnar cells (CBC), were found to give rise to all four intestinal epithelial lineages (Cheng & Leblond, 1974). Other evidence that CBC were stem cells came from subsequent studies which found that single mutated cells gave rise to all intestinal epithelial cell types within a crypt-villus axis (Bjerknes & Cheng, 2002), (Winton & Brooks, 1998). The functional existence of IESC was further demonstrated with evidence that clonally proliferating cells appear to regenerate the intestinal epithelium after complete depletion of the crypts by exposure to high dose irradiation (Potten, 2004). These IESC near the base of small intestinal crypts have been thought to be slowly dividing cells with a cycling time of 24-30 hours compared to progenitor or transit amplifying cells higher up in the crypts that have a cycling time around 12 hours and have more limited capacity for self renewal (Potten & Loeffler, 1990), (Bjerknes & Cheng, 2006). Based on this idea that IESC are slowly dividing, label retaining studies that mark slowly dividing cells which retain their template strand DNA have been used to predict that out of approximately 250 total cells in each small intestinal crypt, only 2 to 6 cells located at cell positions 2-7 from the base of the crypts are label retaining cells (LRC), believed to be IESC (Potten & Booth, 1997). Since a majority of LRC were localized at position +4 from the base of the crypt these have been termed +4 cells.

These studies and characteristics of IESC have led to a concept that there may be two populations of IESC, the '+4' IECS lying above Paneth cells and the CBC lying between Paneth cells, and exemplifies the fact that there is still a need for conclusive evidence to confirm the precise location and identity of IESC. For example, LRC are not solely localized at +4, but are distributed at positions 2-7 from the crypt base, which can include the CBC population. Punitive IESC have also been identified that distinctly mark cells in the +4 IESC or CBC zones. Thus one proposal by Dr. Susan Henning at UNC suggests that upper stem cell zone (USZ) and lower stem cell zone (LSZ) may be better terminology. Many aspects of IESC including their location will remain unverified until valid IESC markers in the USZ and LSZ are defined. It is also important to show multipotency of these IESC *in vitro* as well as *in vivo* for verification that they are true IESC.

IESC Markers

Recently several IESC markers have been proposed which are preferentially expressed in the USZ or LSZ (Figure 1). Indirect evidence that bone morphogenic protein receptor 1a (BMPR1A) and phosphorylated-phosphatase and tensin homolog deleted on chromosome 10 (p-PTEN) are markers of IESC in the USZ has been demonstrated using label retaining assays and mouse knockout models. The phenotype of BMPR1A and PTEN knockouts showed that deregulation of these pathways led to expansion of the IESC zone and an increase in proliferation leading to intestinal polyposis (He et al., 2004), (He et al., 2007). Evidence using microarray analysis of small intestinal crypts and short-term label retaining assays indicated that Doublecortin- and Calmodulin Kinase-Like 1 (DCAMKL1) may represent another

potential IESC marker in the USZ (Giannakis et al., 2006). The microarray from theses same studies identified that Eph receptors could make good candidates for cell surface markers of IESC. This was further strengthened by findings in EphB2 and EphB3 gene deletion models which demonstrated a disruption of cell migration and through characterization of the expression pattern of Eph receptors (Batlle et al., 2002). Some integrins including α2β1 also make good candidates as surface markers of IESC (Beaulieu, 1992). Musashi-1 shows potential as an IESC marker, since Musashi-1 positive cells colocalize with label retaining cells and the proliferation marker Ki67 in the base of crypts (He et al., 2007; Potten et al., 2003). However Musashi-1 staining can often localize to CBC, +4 cells and also cells at positions higher in the crypt then thought to represent IESC. Strong experimental evidence suggests that Lgr5 is a true IESC marker. Both lineage tracing models and *in vitro* pluipotency have demonstrated that Lgr5 positive cells are CBC cells that give rise to all intestinal cell lineages (Barker, van Es, Kuipers, Kujala, van den Born, Cozijnsen, Haegebarth, Korving, Begthel, Peters, & Clevers, 2007a; Sato et al., 2009). Genetic lineage tracing has also been used to show that cells expressing Sox9 give rise to all differentiated cell types in the embryonic intestine {{155 Akiyama,H. 2005; }}. Mice that have a Sox9 gene deletion do not develop Paneth cells suggest that Sox9 is required for Paneth cell differentiation however is not required for the development of the other cell lineages {{156 Mori-Akiyama,Y. 2007; }}. Redundancy in function across the Sox protein family is a common theme and therefore compensatory effects of other SOX proteins could account for differentiation of the other cell lineages in the absence of SOX9 expression {{158 Hoser,M. 2008;159 Matsui,T. 2006; }}. Endogenous SOX9 protein localizes to

the CBC and to cells within the USZ or transit amplifying zones {{157 Blache,P. 2004; }}. Recently, Sox9 transcriptional activity was visualized in the intestine using a $Sox9^{EGFP}$ reporter mouse. Differential expression of $Sox9^{EGFP}$ was observed within the USZ and LSZ. Cells expressing high levels of $Sox9^{EGFP}$ ($Sox9^{EGFPHI}$) where localized to the USZ and to cells on the villus. Further evaluation of these cells revealed that they were post-mitotic or non-proliferating cells with an enteroendocrine phenotype {{116 Formeister,E.J. 2009; }}. Cells expressing low levels of $Sox9^{EGFP}$ ($Sox9^{EGFPLO}$) localized to the LSZ/CBC and these cells were shown to be enriched for Lgr5 and other stem cell markers {{116 Formeister,E.J. 2009; }}. Thus $Sox9^{EGFP}$ may mark terminally differentiated enteroendocrine cells in the USZ, as well as LSC/CBC. A key question is whether the non-dividing enteroendocrine cells expressing high levels of Sox9 in the USZ may in some instances adopt an IESC phenotype. Lineage tracing and reporter mouse models have shown great potential in identifying IESC, but to date the expression pattern of IESC markers has not been fully characterized after injury such as irradiation which creates an ideal model to study IESC and their role in regeneration after complete crypt loss {{12 Potten,C.S. 2004; }}.

Irradiation as a model to study IESC

Irradiation has been valuable in defining many aspects of cells within the intestinal crypts. This injury model is particularly useful for characterizing IESC and their response to injury, because it is a cytotoxic agent that can be precisely controlled and measured and can be uniformly delivered across a tissue region or given as whole body irradiation. In the intestine, this model can be used to eliminate proliferative cells excluding a few clonogenic cells that are capable of regenerating the intestinal

epithelium {{12 Potten,C.S. 2004; }}. A wide range of doses have been tested and have shown that cells within the USZ or +4 zone are highly susceptible to radiation–induced apoptosis which peaks at radiation doses as low as 1Gy and is maximal as early as 4 hours after irradiation. The highest rate of apoptosis is around position 4 above the crypts, but is induced highly throughout the entire crypt base {{144 Potten,C.S. 1998; }}. A recent study compared radiosensitivity of USZ or +4 cells and LSZ/CBC and suggested that LSZ/CBC cells were more resistant requiring a high dose of 10Gy for peak apoptosis (Barker, van Es, Kuipers, Kujala, van den Born, Cozijnsen, Haegebarth, Korving, Begthel, Peters, & Clevers, 2007a). The colon appears to be less sensitive to radiation-induced apoptosis at early time points after irradiation and does not show any region specific apoptosis along the length of the crypt (Cai, Roberts, Bowley, Hendry, & Potten, 1997). Indeed the identity of colon IESC is less well defined than small intestine IESC. Radiation has also been used to show that IESC in the small intestine have a unique ability to protect their genome from mutation {{129 Potten,C.S. 2002; }}. This, along with the high rate of apoptosis in the IESC zone after injury, may present a mechanism by which the small intestine prevents proliferation of genetically damaged cells and maintains an extremely low rate of cancer formation after genotoxic injury. The intestine also seems to be able to effectively recognize the degree of injury because it compensates for increases in induced apoptosis at higher dose of irradiation by increasing regeneration compared to lower doses (Hendry, Roberts, & Potten, 1992). This increase in regeneration as the dose of irradiation is increased suggest that the greater the injury, the more cells are recruited into a clonogenic state to help rescue the epithelium (Potten, Merritt, Hickman, Hall, & Faranda, 1994). Clonogenic cells have

been considered putative IESC, but irradiation may be altering their phenotype and how they compare to IESC before injury has not been established. Combining a high dose irradiation model that shows the greatest increase in clonogenic cells and regeneration, with lineage tracing or reporter mouse models could effectively determine any differences between IESC before and after irradiation.

Mediators of regeneration after irradiation

It is noteworthy that relatively little is known about the local, paracrine or autocrine mediators of regeneration after irradiation. Some studies suggest that endothelial cells may be required for appropriate regeneration after irradiation although this is controversial (Schuller et al., 2007; Wang, Boerma, Fu, & Hauer-Jensen, 2007). Another recent study suggests that the protein, p53 upregulated modulator of apoptosis (PUMA), regulates the radiosensitivity of IESC. PUMA, which works in a p53 dependent manner, was seen to be highly upregulated in the intestine after irradiation and gene deletion of PUMA led to increased regeneration after irradiation. Interestingly, IESC in the USZ appeared to show greater apoptosis then cells in the LSZ (Qiu et al., 2008). However, detection and quantification of cells in the LSZ was limited due to the difficulty in recognizing these slender cells between more prominent Paneth cells.

The $Sox9^{EGFP}$ reporter mouse would provide an effective model to visualize these cells in the LSZ, as well as to quantify the expression of PUMA on the USZ and LSZ and determine the underlying mechanisms regulating PUMA through the isolation of $Sox9^{EGFP}$ cells for molecular analysis. It would be interesting if the increased apoptosis of cells in the USZ was associated with $Sox9^{EGFPHI}$ enteroendocrine cells, which may

identify the importance of these cells in the maintenance of the IESC niche. This is consistent with a previously hypothesized enteroendocrine cell-based quiescent intestinal stem cell niche, which has not been confirmed experimentally (Radford & Lobachevsky, 2006).

Therapies for regeneration

Furthermore, the suppression of PUMA could provide an effective therapy to protect IESC from radiation damage. Insulin-like growth factor-I (IGF-I) suppresses PUMA independently of p53 and could be an effective therapy (Han et al., 2001). IGF-I has also been seen to promote SOX9 expression and survival of SOX9 positive cells after irradiation (Ramocki et al., 2008). In other tissues, IGF-I plays a major role in the survival, expansion and regeneration of stem cells (Arsenijevic, 2005; Ye & D'Ercole, 2006). IGF-I seems to mediate the actions of growth hormone (GH) and GLP2, the only approved or under trial trophic therapies for human intestinal disease, respectively (Dube, Forse, Bahrami, & Brubaker, 2006; Krysiak, Gdula-Dymek, Bednarska-Czerwinska, & Okopien, 2007). However, one complication with using growth factors as therapies for cancer patients undergoing radiation therapy is that they are desensitizing therapies which may protect not only the normal tissue, but also the tumor tissue rendering them ineffective. Interestingly, GH administered before radiation exposure has been seen to protect normal tissue but not implanted adenocarcinoma from irradiation. IGF-I, which is downstream of GH, may be an even more effective therapy, but its effects on tumor risk after irradiation should be established (Morante et al., 2003).

Crypt microcolony assay

Irradiation has also been widely used to test therapies that can protect IESC or increase regeneration {{15 Potten,C.S. 2003; }}. Many of these studies utilize the crypt microcolony assay, which compares the number of regenerating crypts, as defined by a given number of dividing cells, after irradiation in animals with and without treatment (Khan, Shui, Ning, & Knox, 1997)(Booth, Booth, Williamson, Demchyshyn, & Potten, 2004)(Ishizuka et al., 2003). The crypt microcolony assay is an indirect measurement of IESC activity and is often dependent on using a high dose of irradiation that does not allow for analysis of the complete regenerative process due to limited animal survival. Many of the irradiation models that have been used are limited by either using a low dose of irradiation that only eliminates a portion of the IESC population or use of a high dose of irradiation that is limited by poor survival of animals.

Hypothesis

This study focuses on development of a high dose abdominal irradiation model that allows for survival of only IESC that can regenerate the intestine. It is hypothesized that this model will increasing the animal survival rate so that the regenerative response of IESC can be further characterized. This abdominal irradiation model will also used to characterize the expression pattern of the putative IESC marker Sox9. It is further hypothesized that Sox9 will provide a useful marker of IESC during the regenerative process after irradiation.

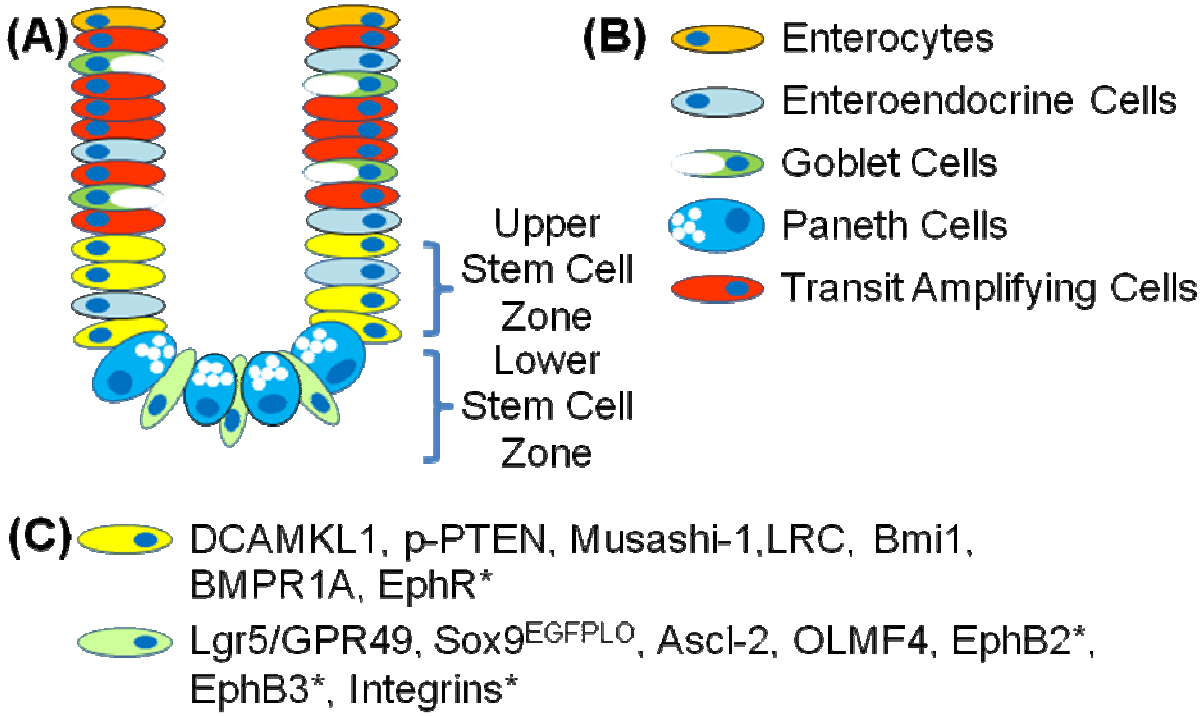

Figure 1: Intestinal cell lineages and intestinal stem cell (IESC) markers. (A) Diagram of an intestinal crypt showing the position of the Upper Stem Cell Zone (USZ) in yellow and Lower Stem Cell Zone (LSZ) in light green. **(B)** Differentiated intestinal cell types. **(B)** Expression pattern of putative IESC markers. * - These proteins show a gradient of expression throughout the IESC zone.

Chapter 2

Methods

Experimental Mice

The mice used in these experiments included wild-type C57BL/6 mice and $Sox9^{EGFP}$ mice. The $Sox9^{EGFP}$ mice were provided by Dr. Scott Magness (University of North Carolina at Chapel Hill). $Sox9^{EGFP}$ transgenics were originally generated for the Gene Expression Nervous System Atlas (GENSAT) BAC Transgenic Project. Frozen embryos were obtained from the Mutant Mouse Regional Resource Center and reconstituted in foster mice as previously described (Gong et al., 2003) within the Mouse Mutant Resource Core at UNC-Chapel Hill. These mice are on a CD-1 background and were genotyped by visualization of enhanced green fluorescent protein (EGFP) expression in tail snips (Formeister et al., 2009).

Abdominal irradiation model

An abdominal irradiation model was developed using the X-RAD 320 irradiator from Precision X-Ray (North Branford, CT) that was fitted to simultaneously irradiate up to 8 mice. The mice were anesthetized with 2% isoflurane throughout the procedure. The lower half of each mouse below the xiphoid process was placed within a 20cm X 20cm irradiation zone, while the upper half was kept outside of this area and was not exposed to irradiation (Figure 2, pg 17). The mice were exposed to a total of 14Gy of irradiation at a rate of 2Gy/minute. After irradiation, the mice were housed in an

isolation cubicle in room 1131 of the Neuroscience Research Building. This is necessary because mice cannot be returned to SPF housing after being removed to another facility.

Tissue Collection

The mice were killed on days 3, 4, 5, 7 and 9 after irradiation. Mice were injected with 5-ethynyl-2'-deoxyuridine (EdU, Invitrogen A10044, Carlsbad, CA) at a concentration of 4µg/g body weight 90 minutes before they were killed. The entire intestine was removed and flushed with PBS. Samples were taken from the duodenum, jejunum, mid-gut, ileum, and proximal and distal colon for histology or biochemical analyses. Samples for protein or RNA were snap frozen in liquid nitrogen and stored at -80ºC. Samples for histology or immunostaining were fixed for 24 hours in 4% paraformaldehyde (PFA) freshly made in PBS. These samples were then cryo-protected in 10% sucrose for 24 hours followed by 30% sucrose for 24 hours. The samples were then embedded in Optimal Cutting Temperature (OCT) medium, frozen on dry ice and stored at -80ºC. Tissue sections were cut at 6-10µm thickness and placed on positively charged slides for histology or immunostaining.

Histology and detection of proliferating cells

To visualize histology, tissue sections were stained with hematoxylin and eosin (H&E) by Kirk McNaughton (Cell and Molecular Physiology Department, UNC-Chapel Hill). For immunofluorescence, sections were first washed twice in 0.05 M Tris to for three minutes each time remove the OCT. All washes were done in 0.05 M Tris for three minutes each.

Proliferating cells were detected based on incorporation of EdU into newly synthesized DNA or immunostaining for Ki67. EdU assays use a two-step click reaction that is based on detection of incorporated EdU with an Alexa Fluor® azide dye (Alexa Fluor® 488) which gives green fluorescence, or Alexa Fluor® 594 which gives red fluorescence (Click-iT™ EdU Alexa Fluor® 488 and 594 Imaging Kits, Invitrogen, Carlsbad, CA). EdU contains a small alkyne group that is detected by an azide containing fluorescent dye. EdU offers advantages over commonly used BrdU based methods. Because the Alexa Fluor® dye is small, only mild permeabilization is required to detect incorporated nucleotide. No DNA denaturation or antibody-based detection is needed which makes the system faster and more compatible with dual labeling for other proteins. EdU was detected following manufacturers instructions through steps 3.3 – 4.6 (see Table 1, pg 18). Ki67 was detected by immunofluorescence as outlined below.

Immunohistochemistry

If sections were first stained for EdU, primary antibodies were added directly after removal of Alexa fluor dye and the final wach of the Click-iT™ procedure. If EdU staining was not perfomed, the sections were treated with 0.05 M Tris-Triton-X 100 (TT) buffer, washed twice, and incubated in 5% Normal Goat Serum in PBS+0.3% Triton-X 100 (blocking medium) for 30 min at room temperature. Primary antibodies were added to the sections in Dako Antibody Diluent (Dako, S0809, Carpinteria, CA) for 12 hours at 4ºC at the following dilutions, anti-SOX9 (rabbit, 1:1,000, no. AB5535; Chemicon, Temecula, CA), anti-substance P (rat; 1:100, no. MAB356; Chemicon), anti-lysozyme (rabbit, 1:1,000, no. RP 028; Diagnostics Biosystems, Pleasanton, CA) and anti-Ki67 (mouse, 1:100, no. M7249; Dako, Carpinteria, CA). Detection of Ki67 required antigen

retrieval after the initial wash steps by incubating the sections at 125ºC for 30 seconds followed by 90ºC for 10 seconds in Reveal Decloaker RTU (no. RV1000MMRTU; Biocare Medical, Concord, CA). These samples were then moved into PBS for 20 minutes at room temperature. After primary antibody incubation, sections were washed 3 times and secondary antibodies were added at the following concentrations, anti-Rabbit- Alexafluor 488 (1:500, no. Z-25302, Molecular Probes, Eugene, OR), anti-Rabbit-594 (1:250; no. 711-505-152 Jackson Immunoresearch Laboratories, West Grove, PA) and anti-Rat-594 (1:250; no. 712-505-150 Jackson Immunoresearch Laboratories, West Grove, PA). Ki67 required amplification using anit-Mouse IgG-Biotinylated (1:200; Jackson Immunoresearch Laboratories, West Grove, PA) followed by Alexafluor-555-labeled streptavidin (1:250, no. S32355, Molecular Probes). Sections were then washed 3 times and nuclei were stained with Bisbenzamide (1:20000) and Draq5 (1:1000 no. BOS-889-001; Biostatus, San Diego, CA) in Tris for 10 min. This was followed by a 5 minute wash and then the slides were cover slipped using Hydromount (National Diagnost, no. HS-106, Atlanta, GA).

A major goal of these studies was to assess if Sox9 marked proliferating cells in microcolonies and regenerating crypts between days 3 – 9 after irradiation. Thus the localization of immunoreactive Sox9 was compared with Ki67 or EdU on the same sections.

Quantification of Sox9^{EGFP}

To assess the effects of radiation on regeneration of Sox9^{EGFP} putative stem cells, Sox9^{EGFP} was directly visualized at days 3 – 9 after radiation. Prior studies

(Formeister 2009) indicate two populations of $Sox9^{EGFP}$ cells defined by high expression, $Sox9^{EGFPHI}$, and low expression, $Sox9^{EGFPLO}$. In normal, uninjured small intestine, $Sox9^{EGFPHI}$ cells in crypt and villus appear to represent post-mitotic cells expressing enteroendocrine markers. $Sox9^{EGFPLO}$ are localized to the base of the crypts at locations thought to represent multipotent stem cells (Formeister 2009). Thus, the number of $Sox9^{EGFPHI}$ and $Sox9^{EGFPLO}$ cells was counted in 15 crypts of jejunum on 3 slides per mouse at days 3, 5, and 9 to assess if there was differential expansion of $Sox9^{EGFPHI}$ and $Sox9^{EGFPLO}$ cells during regeneration. In addition, localization of $Sox9^{EGFP}$ was compared with immunostaining for substance P (an enteroendocrine marker) or lysozyme (a Paneth cell marker) to assess if $Sox9^{EGFP}$ was expressed in these differentiatied lineages.

Figure 2: Mouse placement in the X-RAD 320 from Precision X-Ray. Each mouse is kept anesthetized with its head placed in an open syringe connected to a continuous tube supplying 2% isoflurane. The lower half of each mouse is placed within the irradiation zone specified by the illuminated area.

Permeabilization	Remove the wash solution. Add 1 ml 0.5% Triton® X-100 in PBS and incubate for 20 minutes at room temperature.
EdU Detection	Prepare 1X Click-iT™ EdU buffer additive by diluting the 10X solution in deionized water. Prepare this solution fresh and use the solution on the same day.
	Preparation of Click-iT™ reaction cocktail. Adjust to the volume neede 1X Click-iT™ reaction buff er – 86uL CuSO4 – 4uL Reaction buff er additive – 10uL Alexa Fluor® azide – 0.25uL Total Volume – 100.25uL
	Remove the permeabilization buffer (step 3.3) and wash cells twice with 1 mL 3% BSA in PBS. Remove the wash solution.
	Add Click-iT™ reaction cocktail.
	Incubate for 30 minutes at room temperature, protected from light.
	Remove the reaction cocktail and wash once with 1mL 3% BSA in PBS. Remove the wash solution.

Table 1: Outline of the protocol for EdU detection of proliferating cells.

Chapter 3

Results

Body weight and survival

Figures 3A and 3B (pg 27) show body weights and survival rates for CD1 and C57BL/6 mice used in this study. CD1 mice showed 100% survival out to 9 days, the latest time point tested to date. Survival of C57BL/6 mice was slightly less although 80% of animals survived up to day 7. To date we have not extensively tested C57BL/6 mice through the 9 day time point. Both CD1 and C57BL/6 mice lost weight after irradiation. Peak loss for C57BL/6 mice occurred at day 5 and animals began to regain weight by day 7. After initial weight loss at day 5, CD1 mice maintained body weight through day 9. The high survival rates and increased or maintained body weights of C57BL/6 and CD1 mice through days 7 – 9 indicate that the abdominal irradiation model will be valuable for assessing crypt regeneration and effects of irradiation on stem cells through and beyond day 9.

Regional effects of abdominal radiation on crypt damage and regeneration

Abdominal irradiation of mice at a dose of 14Gy resulted in a differential response throughout the small intestine and colon. Figures 4 – 8 show H&E stained sections of duodenum, jejunum, and ileum from non-irradiated mice (Figure 4, pg 28-29)

and mice at 3 (Figure 5, pg 30-31), 5 (Figure 6, pg 32-33), 7 (Figure 7, pg 34-35), and 9 (Figure 8, pg 36-37) days after irradiation. The duodenum showed the least tissue damage and had a regenerative response as early as day 3 after irradiation (Figures 4A and 5A, pg 30-33). This was followed by an increasing hyperplastic response characterized by deep, densely staining hyper-regenerative crypts from days 5 through 9 (Figures 6A, 7A and 8A, pg 32-37). The duodenum then showed almost complete recovery to a normal physiological state, although with some remaining areas of regeneration and crypt fission, by day 9 (Figure 8A, pg 36-37). In the jejunum, there was almost complete crypt loss with the appearance of a few small regenerative crypts and sub-epithelial microcolonies at day 3 after irradiation (Figure 4B and 5B, pg 28-31). There were increasing numbers of hyper-regenerative crypts that continued to expand from days 5 through 9 (Figure 6B, 7B and 8B, pg 32-37). At day 9, there was recovery of the villi, but the crypts continued to show a hyperplastic response demonstrated by an increase in cell number and size (Figure 8B, pg 36-37). The ileum showed the greatest tissue damage with fewer, shortened villi and almost no crypts at day 3 (Figures 4C and 5C, pg 28-31). A regenerative response demonstrated by a recovery in the number of villi and hyperplastic crypts was seen at day 5 (Figure 6C, pg 32-33). This was followed by the appearance of hyper-regenerative crypts and varying recovery of villi at days 7 and 9 after irradiation (Figure 7C and 8C, pg 34-37).

The subsequent analysis of intestinal stem cells (IESC) in small intestine was focused on the jejunum due to the ideal injury response to irradiation characterized by crypt loss, proliferating IESC and microcolony formation by day 3, followed by regeneration and subsequent hyper-regeneration that has been used in previous

studies. This process is a useful injury and regeneration model for the study of stem cells, because the intestinal crypts have been lost due to massive apoptosis and regeneration is believed to be mediated by a few multipotent clonogenic stem cells that go on to regenerate the intestinal crypts and epithelium (Potten, 2004).

Figure 9 (pg 38) shows the response of the proximal and distal colon to 14Gy abdominal irradiation. Neither proximal nor distal colon showed complete crypt loss. Crypt damage was evident at days 3 and 5, being more apparent in the distal colon. In both proximal and distal colon there was the appearance of large hyper-regenerative crypts by day 7 with adjacent regions showing continued evidence of crypt loss.

A subset of proliferating cells express SOX9 protein during crypt regeneration after irradiation

The effects of irradiation on proliferation were analyzed with the markers of proliferation Ki67 and EdU. Ki67 marks actively cycling cells while EdU detects only cells in S-phase of the cell cycle. Expression of SOX9 and Ki67 was compared on the same sections to test if SOX9 marks proliferating cells. In non-irradiated intestine SOX9 was strongly localized to cells at the crypt base. Ki67 marked a few of these cells at the crypt base and strongly labeled cells higher in the crypts, believed to be progenitor or transit amplifying cells. At day 3 after irradiation, very few Ki67 and SOX9 positive cells were localized to sub-epithelial areas, indicative of microcolonies of regenerating stem cells. At days 4 and 5, there was an expansion of Ki67 immunostaining throughout regenerative areas and hyper-regenerative crypts (Figure 10, pg 39-40). The robust increase of proliferative cells in hyper-regenerative crypts after high dose irradiation is

consistent with previous studies and the hypothesis of increased stem/multipotent cell recruitment after high dose irradiation (Hendry et al., 1992). SOX9 and Ki67 were colocalized to a subset of regenerating cells in hyper-regenerating crypts. There were also SOX9 and Ki67 positive cells that did not co-label. This could be reflective of the observation that SOX9 marks non-cycling enteroendocrine cells that would not be positive for Ki67 and Ki67 marks transit amplifying cells that are not positive for SOX9.

Figures 11 and 12 (pg 41-43) show SOX9 and Ki67 localization in non-irradiated colon and colon through days 3 – 7 after irradiation. In proximal colon of non-irradiated mice SOX9 positive cells were located at the base of the crypts. Most Ki67 cells did not overlap with SOX9 although weak Ki67 staining appeared to co-localize with SOX9 in some cells at the crypt base. In hyper-regenerative crypts at days 5 and 7 there was clear overlap between some strongly labeled Ki67 cells and SOX9. At day 3, SOX9 positive cells at the crypt base did not label with Ki67 while at day 7 hyper-regenerative crypts showed clear co-staining for Ki67 and SOX9, although there was not complete overlap. Figure 10 (pg 39-40) shows data for distal colon. In non-irradiated colon, SOX9 was localized to cells at the crypt base and there was clear overlap between a subset of these cells and Ki67 staining. On day 3, Ki67 staining was less obvious. However, in hyper-regenerative crypts at days 5 and 7 there was expansion of the SOX9 positive cells at the base (day 5) and throughout hyper-regenerative crypts (day 7) and virtually all of these co-labeled with Ki67.

To further determine if cells in the jejunum expressing SOX9 were actively proliferating, co-immunostaining for SOX9 and EdU were evaluated in jejunum (Figure13, pg 44-45). At day 3 after irradiation, colocalization was seen in

microcolonies and sub-epithelial areas. At later time points, SOX9 colocalized with EdU in regenerative areas and hyper-regeneratative crypts (Figure13, pg 44-45). SOX9 was observed to colocalize with only a subset of EdU positive cells. The subset of co-staining cells was limited to small microcolonies at day 3 and at the base of the hyper-regenerating crypts at later time points. This provides indirect evidence that SOX9 may mark early multipotent regenerating stem cells rather than proliferating cells at higher locations in the crypt.

Sox9^{EGFP} expression after irradiation

The Sox9^{EGFP} reporter mouse was used to further analyze the expression pattern of Sox9 after radiation-induced injury and during regeneration. The Sox9^{EGFP} reporter mice breed normally and the EGFP transgene does not cause any negative phenotype as described by Formeister (Formeister, 2009). Consistent with findings of Formeister, non-irradiated jejunum showed Sox9^{EGFPLO} cells at the crypt base and Sox9^{EGFPHI} cells at higher levels in the crypts and on the villi (Figure 14, pg 46). At day 3 after irradiation, Sox9^{EGFP} was expressed at the very base of villi and in some sub-epithelial groups of cells that may represent microcolonies. High expressing Sox9^{EGFP} (Sox9^{EGFPHI}) cells were identified at day 3, while low expressing Sox9^{EGFP} (Sox9^{EGFPLO}) cells were not detectable (Figure 14, pg 46). Throughout hyper-regenerative crypts at days 5 and 7 after irradiation, there was a robust expansion of Sox9^{EGFPLO} cells with few Sox9^{EGFPHI} cells being detected in most crypts (Figure 14, pg 46).

Sox9^{EGFPLO} and Sox9^{EGFPHI} cells in the crypts of non-irradiated mice and mice at days 3, 5 and 9 after irradiation were counted to assess if there were changes in the

number of Sox9^{EGFP} cells in normal crypts compared to regenerative and hyper-regenerative crypts (Figure 15, pg 47). Sox9^{EGFP} could not be counted at day 7 due to technical reasons. There were no crypt structures identified at day 3 after irradiation and, therefore, the number of Sox9^{EGFP} cells per crypt could not be quantified at that time. Additionally, Sox9^{EGFPHI} cells were present in sub-epithelial areas that could not be identified as crypts at day 3. In regenerative crypts at days 5 and 9 after irradiation, no change occurred in the mean number of Sox9^{EGFPHI} cells compared to crypts in non-irradiated mice. Sox9^{EGFPLO} cells could not be found at day 3 after irradiation. At day 5 after irradiation, the number of Sox9^{EGFPLO} cells increased almost three-fold in hyper-regenerative crypts. The number of Sox9^{EGFPLO} cells returned to just above non-irradiated numbers in crypts at day 9 (Figure 15, pg 47). The expansion of Sox9^{EGFPLO} cells provides indirect evidence that they play an important role in the regenerative process.

It should be noted that while there was not an expansion in the mean number of Sox9^{EGFPHI} cells per crypt at days 5 and 9, there was the appearance of occasional large crypts with greater numbers of Sox9^{EGFPHI} cells (Figures 16A, pg 48). This suggests that local factors within individual crypts during regeneration may dictate the regeneration of Sox9^{EGFPHI} cells.

The cell counting data of Sox9^{EGFPHI} and Sox9^{EGFPLO} should be considered as a preliminary qualitative-semi-quantitative test of the patterns of regeneration of Sox9^{EGFPHI} and Sox9^{EGFPLO} cells after irradiation. This reflects the fact that additional numbers of animals and samples need to be studied at each time point. The Sox9^{EGFP} colony has recently been expanded to permit these additional analyses. Furthermore,

the quantitative data need to be captured from tissue sections prepared soon after tissue collection and with samples mounted on the same slide. This is because there was variation in the intensity of $Sox9^{EGFP}$ across slides. Additionally, given the dramatic expansion in $Sox9^{EGFP}$ cells between days 3 and 4, future studies should include evaluation of day 4. It should be noted however that preliminary FACS analysis for GFP provides confirmatory evidence that $Sox9^{EGFPLO}$ cells are expanded at day 5 after irradiation (Van Landeghem and Magness personal communication).

Colocalization of $Sox9^{EGFPHI}$ cells and Substance P

$Sox9^{EGFPHI}$ cells have previously been shown to be mature/post-mitotic enteroendocrine cells, because these $Sox9^{EGFPHI}$ cells colocalized with the enteroendocrine cell markers Substance P and Chromogranin-A but not with Ki67 or the secretory/enteroendocrine progenitor marker, Neurogenin3 (Formeister et al., 2009). Substance P immunostaining was used to determine if $Sox9^{EGFPHI}$ cells exhibit enteroendocrine phenotype after irradiation. At day 3, colocalization of Substance P was detected in a majority of $Sox9^{EGFPHI}$ cells (Figure 16, pg 48). Thus, even in hyper-regenerative crypts, $Sox9^{EGFPHI}$ cells were immunopositive for an enteroendocrine marker. It will be of interest to compare EdU and Substance P staining in the same crypts to assess if these cells are post-mitotic. Note that Figure 16A shows an example of a hyper-regenerative crypt with multiple $Sox9^{EGFPHI}$ and Substance P labeled cells at day 5 contrasting with a crypt composed almost solely of $Sox9^{EGFPLO}$ cells at day 7.

$Sox9^{EGFP}$ and the Paneth cell marker Lysozyme

Previously, two populations of Lysozyme positive Paneth cells have been observed that exist at a 1:1 ratio, one with and one without SOX9 protein; however, $SOX9^{EGFP}$ is not associated with Lysozyme positive Paneth cells which appear to be CBCs between Paneth cells (Formeister et al., 2009). $SOX9^{EGFP}$ was evaluated after Lysozyme immunofluorescence staining to determine if this remained true after irradiation. At day 3 after irradiation, Lysozyme positive cells had lost their normal granulated appearance and the staining seemed more diffuse throughout the cytoplasm (Figure 17B, pg 49). This may be because the cells were releasing their lysozyme-containing granules or because they are apoptotic, which can be further evaluated with Caspase-3 staining (Marshman, Ottewell, Potten, & Watson, 2001). The Lysozyme positive cells at day 3 did not colocalize with $SOX9^{EGFP}$ (Figure 17C, pg 49). At days 5 and 7 after irradiation, Lysozyme immunostaining returned to a more granulated appearance with a few Lysozyme positive cells existing mostly around the base of hyper-regenerative crypts (Figure 17B, pg 49). The majority of $Sox9^{EGFP}$ cells clearly did not colocalize with Lysozyme, however colocalization should be evaluated by confocal microscopy. The robust increase in $Sox9^{EGFPLO}$ cells in hyper-regenerative crypts at days 7 – 9 was not accompanied by a visual increase in Lysozyme positive Paneth cells. At day 9 after irradiation there was a recovery of more normal appearing Lysozyme positive cells at the base of the crypts that appeared largely distinct from $Sox9^{EGFPLO}$ or $Sox9^{EGFPHI}$ cells (Figure 17B, pg 49). Thus, it appears that cells expressing $Sox9^{EGFP}$ are distinct from Lysozyme expressing cells. However, without further analysis with confocal microscopy we cannot entirely exclude the possibility that some Lysozyme positive cells express $Sox9^{EGFP}$.

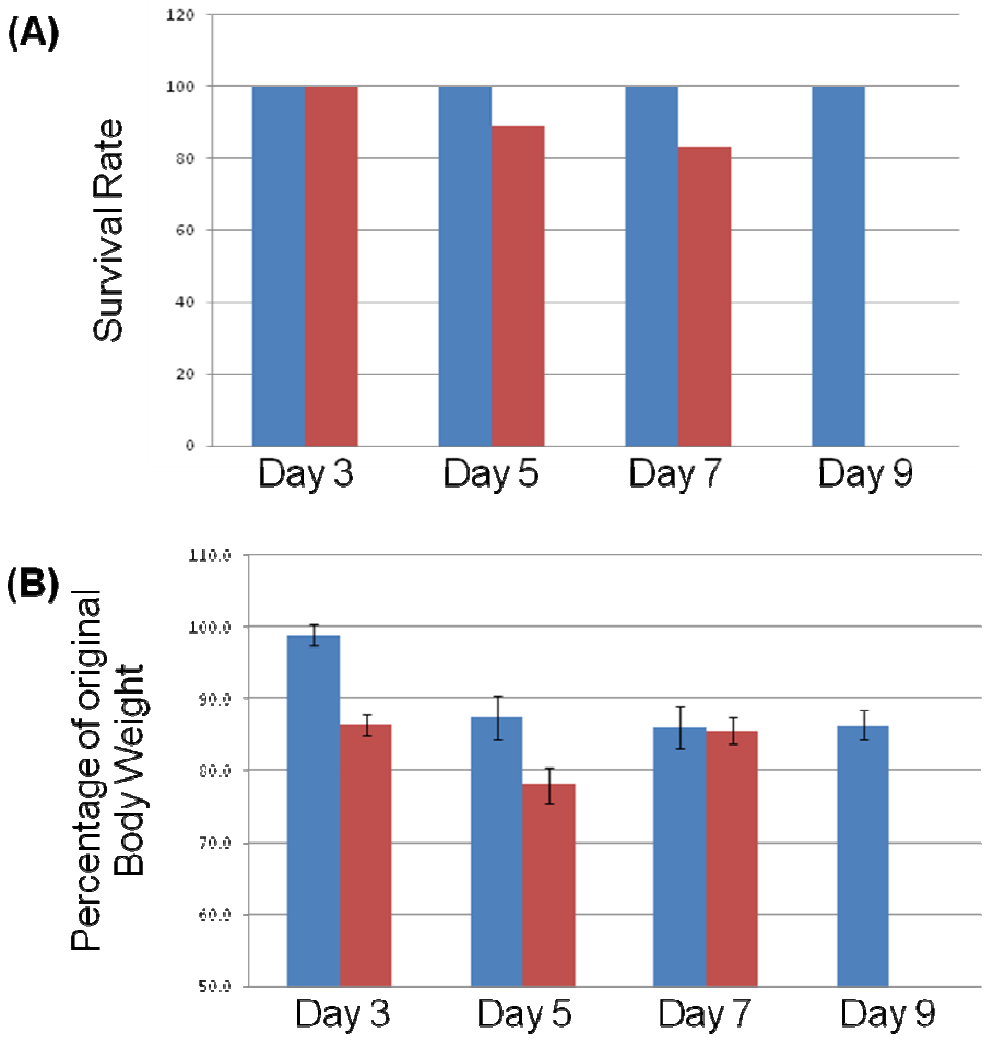

Figure 3: Body weights and survival rates for CD1 and C57BL/6 mice. (A) Survival rates of CD1 (blue bars) and C57BL/6 (red bars) after irradiation. N=7, 5, 3 and 2 for CD1 mice and N=11, 9 and 6 for C57BL/6 mice for each day after irradiation respectively. The decrease in n at each time point is the result of experiment use of mice at each time point, not death due to injury. **(B)** Body weights of CD1 (blue bars) and C57BL/6 (red bars) after irradiation. N=7, 5, 3 and 2 for CD1 mice and N=11, 9 and 5 for C57BL/6 mice for each day after irradiation respectively. The standard error of the mean is shown.

(A)

(B)

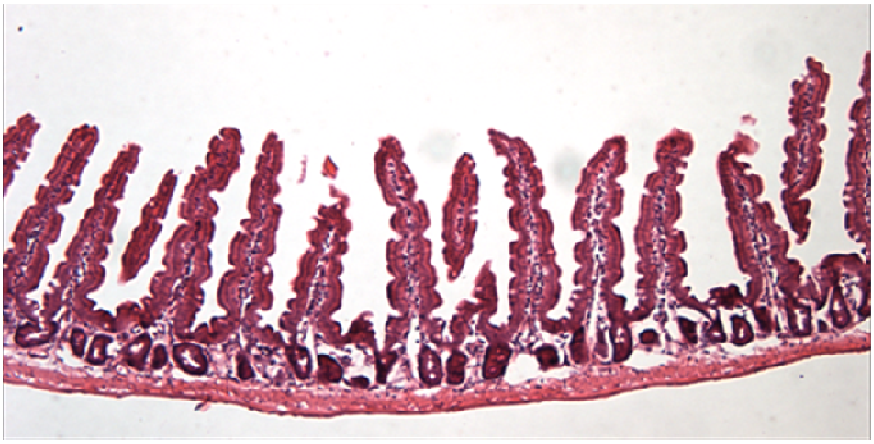

(C)

Figure 4: Normal Small Intestinal Physiology. H&E staining of non-irradiated small intestinal photographed at 5X magnification. (A) Duodenum **(B)** Jejunum **(C)** Ileum

(A)

(B)

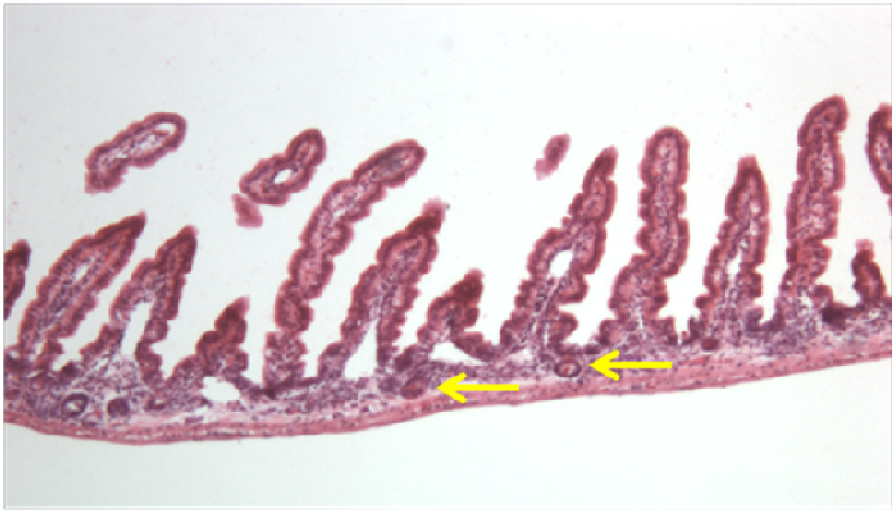

(C)

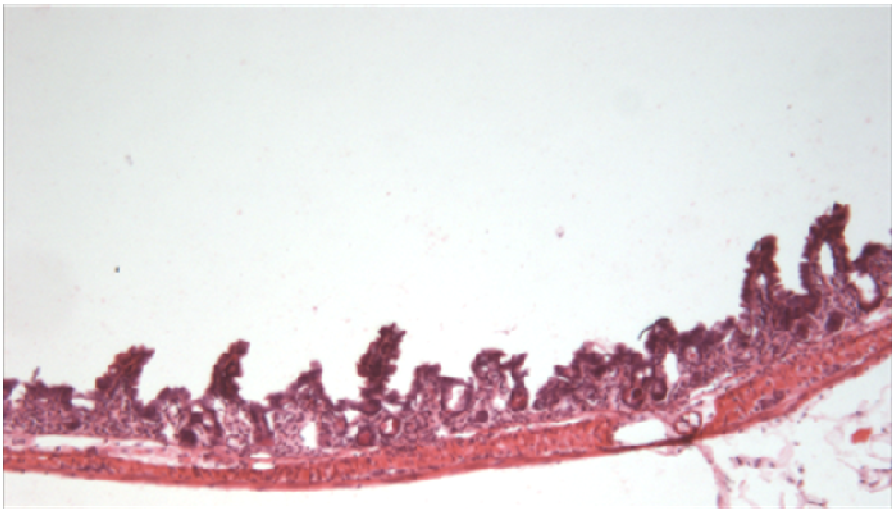

Figure 6: Small Intestinal Damage at day 3 after irradiation. H&E staining photographed at 5X magnification. (A) Duodenum with arrow showing regenerative crypt **(B)** Jejunum with arrows to mirocolonies **(C)** Ileum showing villi and crypt loss

(A)

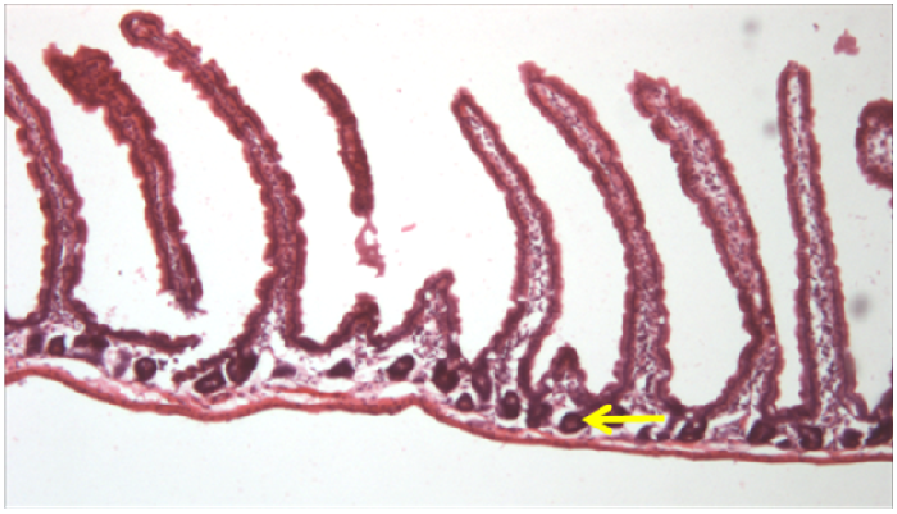

(B)

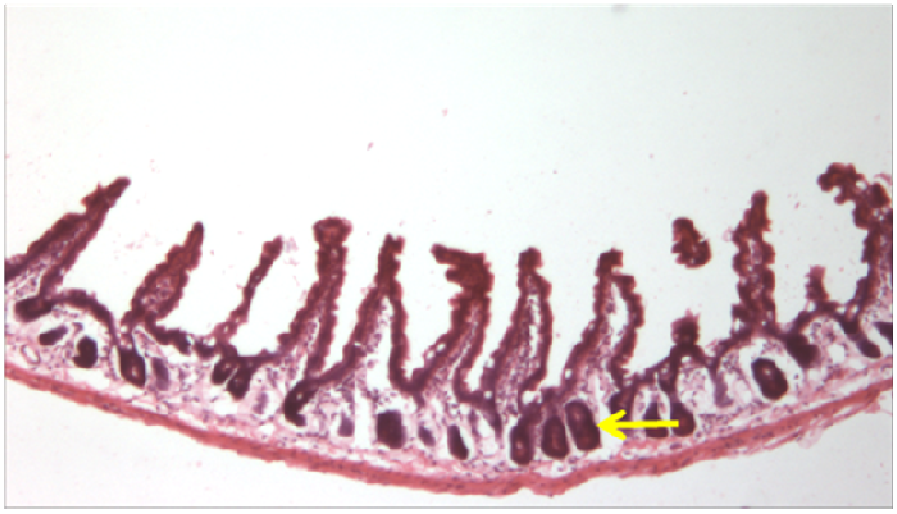

(C)

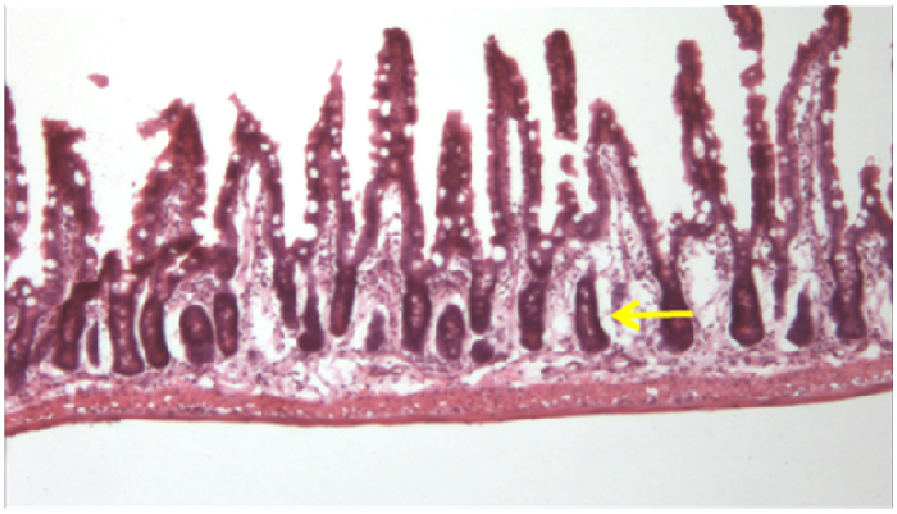

Figure 6: Regenerative response in the small intestine at day 5 after irradiation. H&E staining photographed at 5X magnification. Arrows point to regenerative crypts (A) Duodenum **(B)** Jejunum with recovery of crypts **(C)** Ileum showing recovery of villi and crypts

(A)

(B)

(C)

Figure 7: Hyper regenerative response at day 7 after irradiation. H&E staining photographed at 5X magnification. Arrows show examples of hyper-regenerative crypts that have an increase in size and cell density (A) Duodenum with an increase in the number of hyper-regenerative crypts **(B)** Jejunum with increasing regenerative crypts **(C)** Ileum with hyper-regenerative crypts and disorganized recovery to irradiation

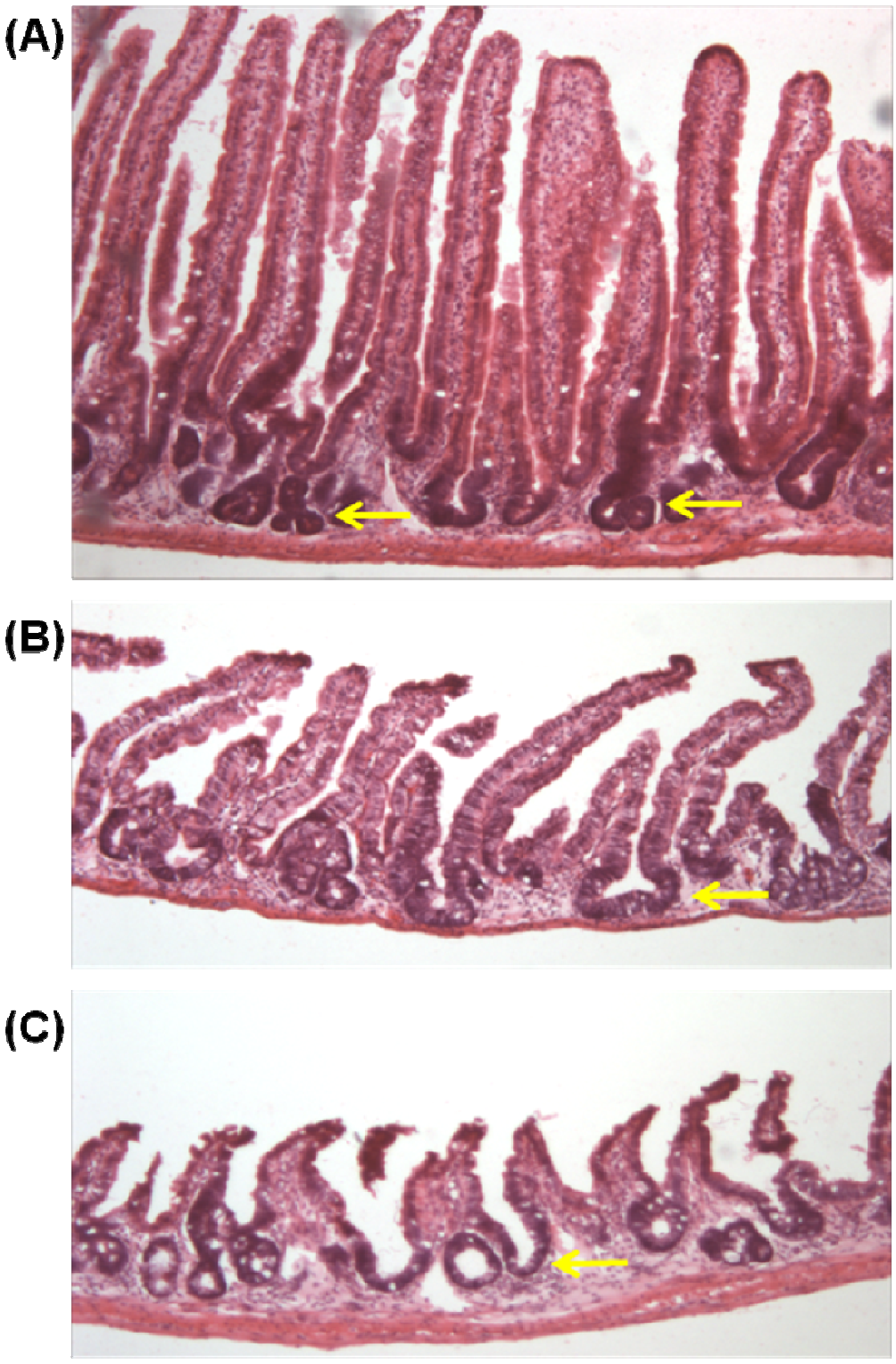
(A)
(B)
(C)

Figure 8: Increase in regeneration and crypt fission at day 9 after irradiation. H&E staining photographed at 5X magnification. Arrows show areas of crypt fission in the duodenum and jejunum as well as regeneration in the ileum. (A) Duodenum **(B)** Jejunum **(C)** Ileum

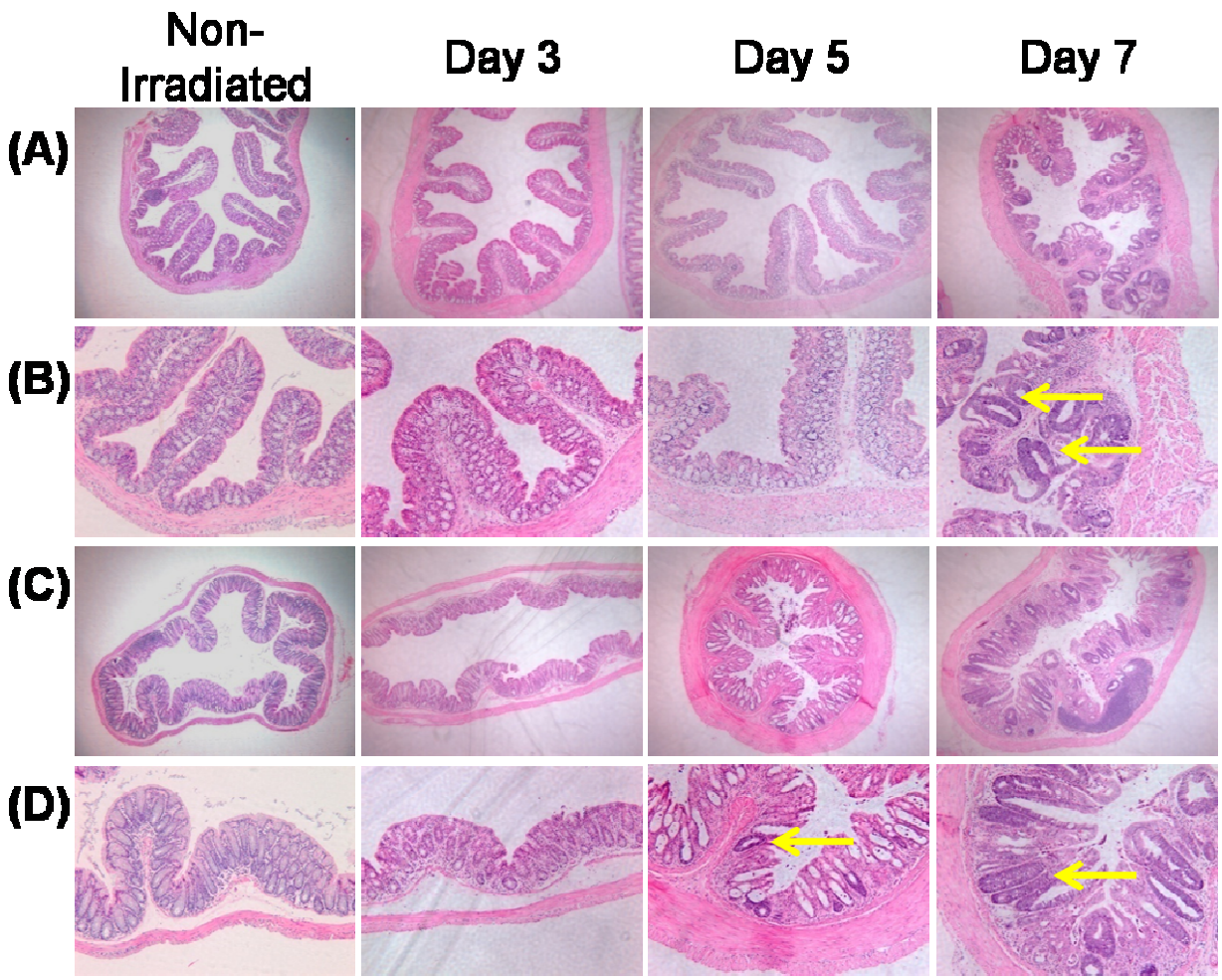

Figure 9: Colon has shorted crypts followed by areas of regeneration after irradiation. H&E staining photographed at 4X and 10X magnification.. Arrows show areas of regeneration. (A) Proximal colon at 4x. **(B)** Proximal colon at 10x. **(C)** Distal colon at 4X. **(D)** Distal colon at 10X.

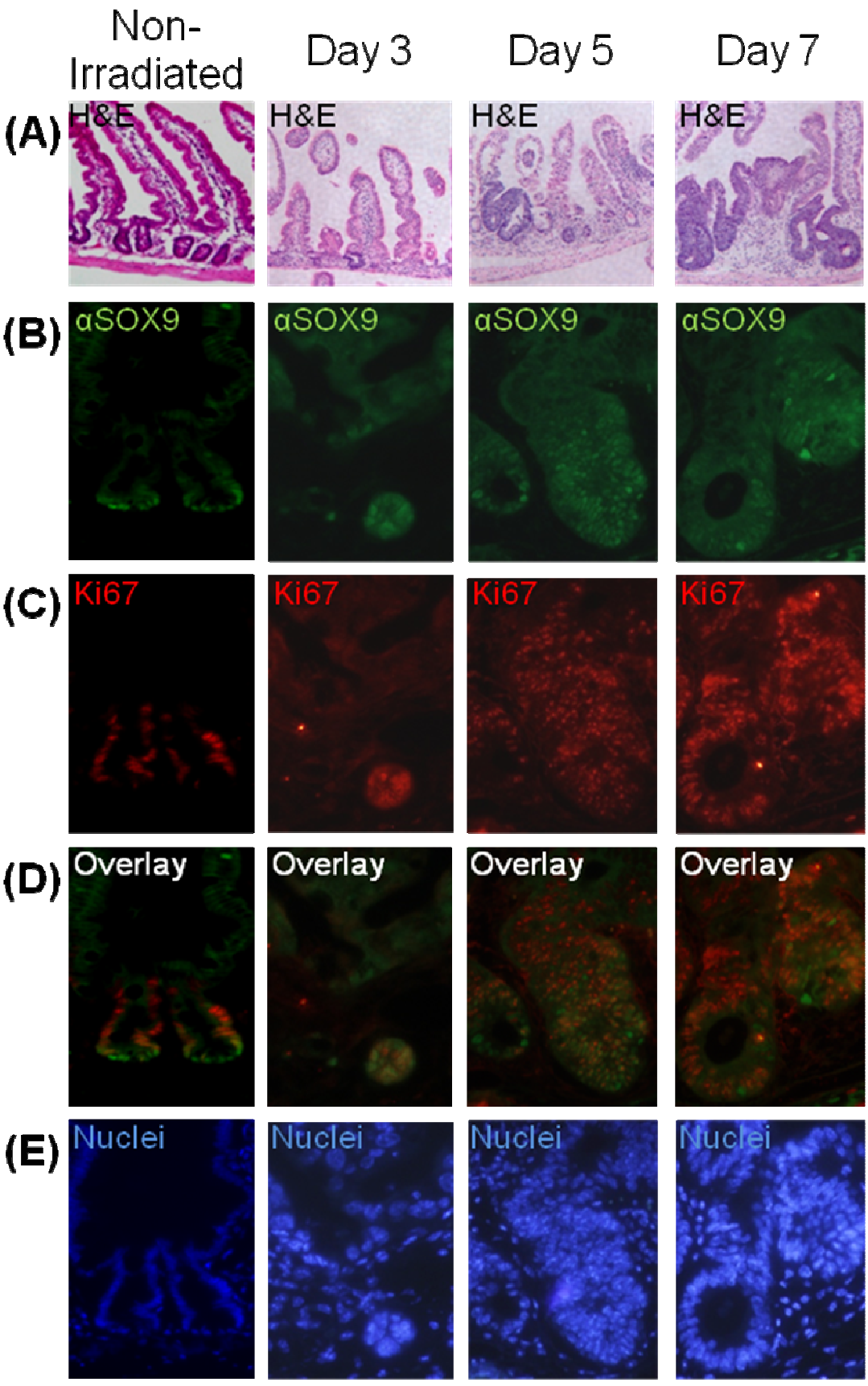
Non-Irradiated
Day 3
Day 5
Day 7
(A)
H&E
H&E
H&E
H&E
(B)
αSOX9
αSOX9
αSOX9
αSOX9
(C)
Ki67
Ki67
Ki67
Ki67
(D)
Overlay
Overlay
Overlay
Overlay
(E)
Nuclei
Nuclei
Nuclei
Nuclei

Figure 10: SOX9 protein and Ki67 colocalize in microcolonies and hyper-regenerative areas after irradiation. (A) H&E staining at higher magnification in areas representative of immunofluorescence staining. **(B)** SOX9 protein (SOX9) in green. **(C)** Ki67 staining in red. **(B)** SOX9 protein (SOX9) staining in green shows colocalization with Ki67 in red. **(C)** Nuclear staining in blue.

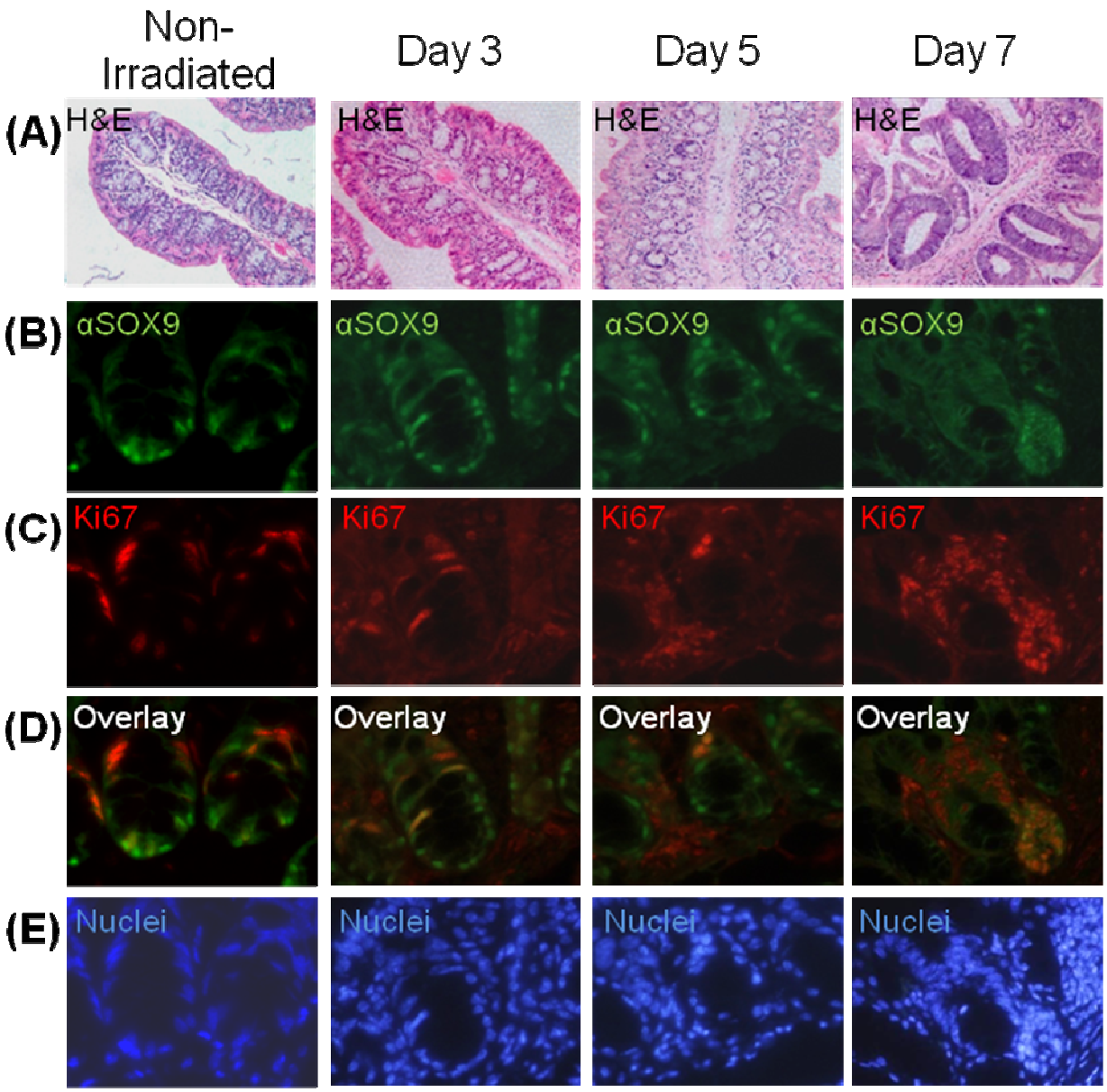

Figure 11: SOX9 protein and Ki67 colocalize in crypts of proximal colon. (A) H&E staining at higher magnification in areas representative of immunofluorescence staining. **(B)** SOX9 protein (SOX9) in green. **(C)** Ki67 staining in red. **(B)** SOX9 protein (SOX9) staining in green shows colocalization with Ki67 in red. **(C)** Nuclear staining in blue.

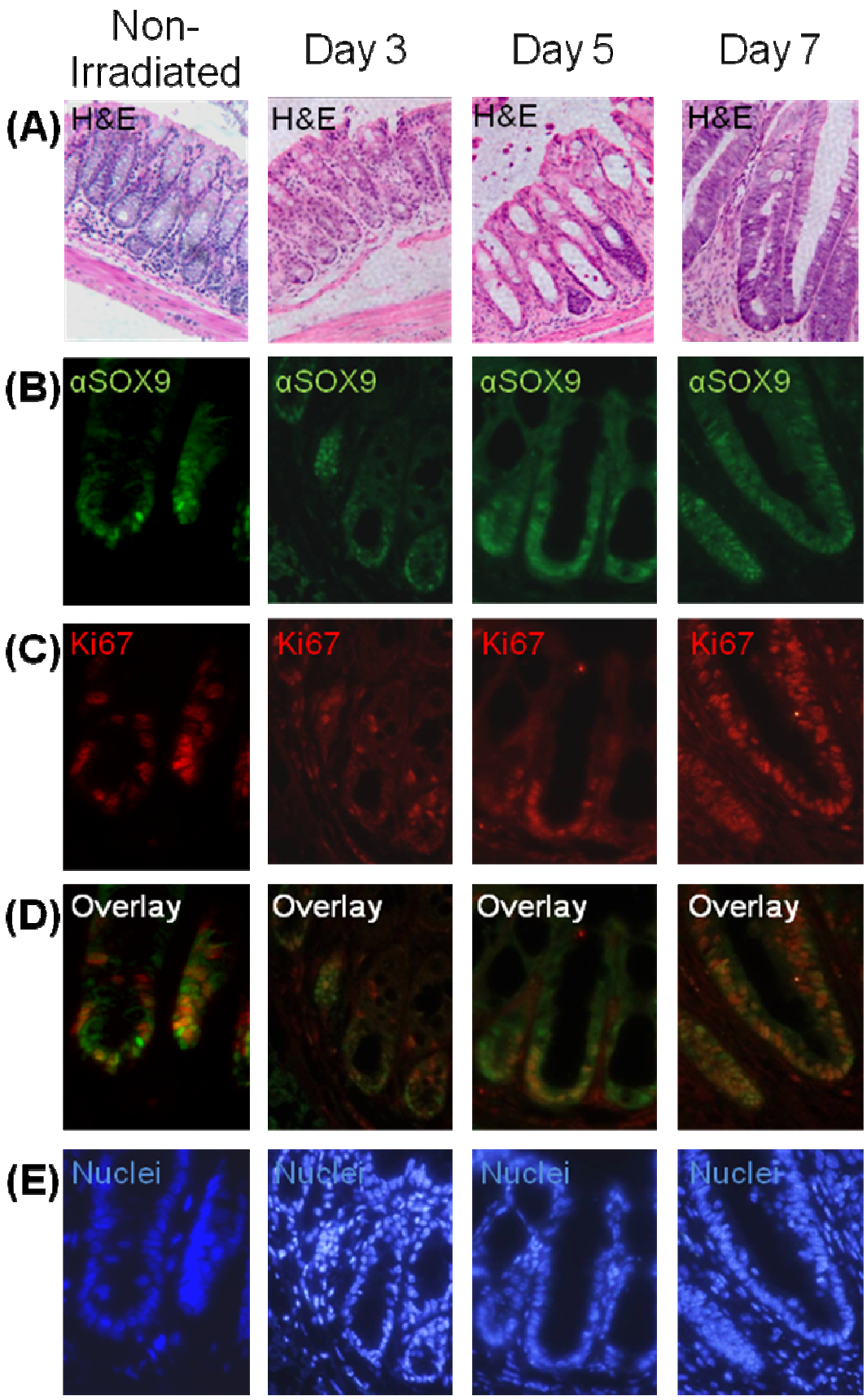
Non-Irradiated
Day 3
Day 5
Day 7
(A)
H&E
H&E
H&E
H&E
(B)
αSOX9
αSOX9
αSOX9
αSOX9
(C)
Ki67
Ki67
Ki67
Ki67
(D)
Overlay
Overlay
Overlay
Overlay
(E)
Nuclei
Nuclei
Nuclei
Nuclei

Figure 12: SOX9 protein and Ki67 colocalization in crypts of distal colon. (A) H&E staining at higher magnification in areas representative of immunofluorescence staining. **(B)** SOX9 protein (SOX9) in green. **(C)** Ki67 staining in red. **(B)** SOX9 protein (SOX9) staining in green shows colocalization with Ki67 in red. **(C)** Nuclear staining in blue.

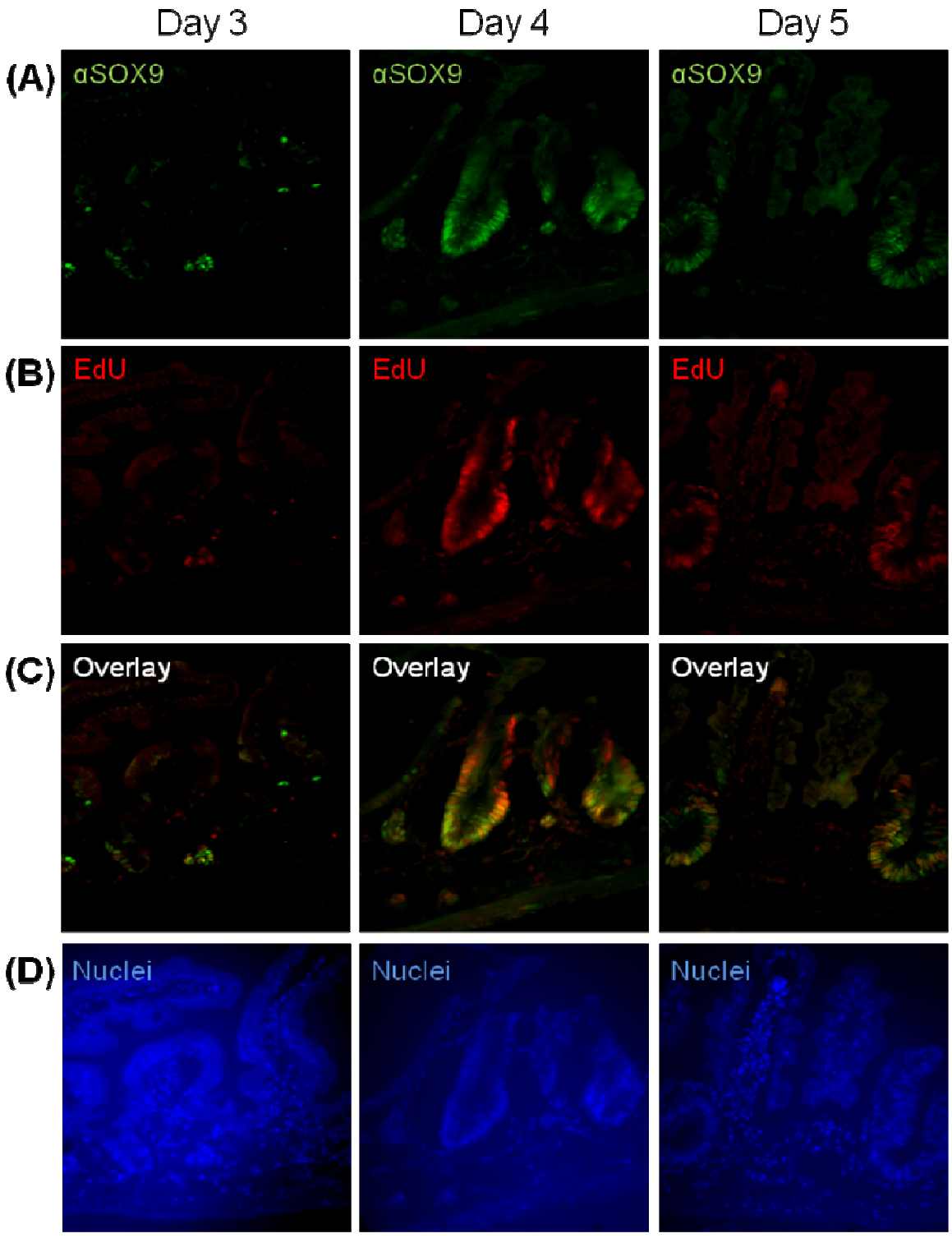
Day 3
Day 4
Day 5
(A)
αSOX9
αSOX9
αSOX9
(B)
EdU
EdU
EdU
(C)
Overlay
Overlay
Overlay
(D)
Nuclei
Nuclei
Nuclei

Figure 13: SOX9 protein colocalizes with a subset of EdU positive cells in sub-epithelial areas and at the base of hyper-regenerative crypts. (A) SOX9 protein (SOX9) staining in green. **(B)** EdU staining in red **(C)** Overlay of SOX9 and EdU showing colocalization in sub-epithelial areas at day 3 and at the base of hyper-regenerative crypts at days 4 and 5. **(D)** Nuclear staining in blue corresponding to the pictures above.

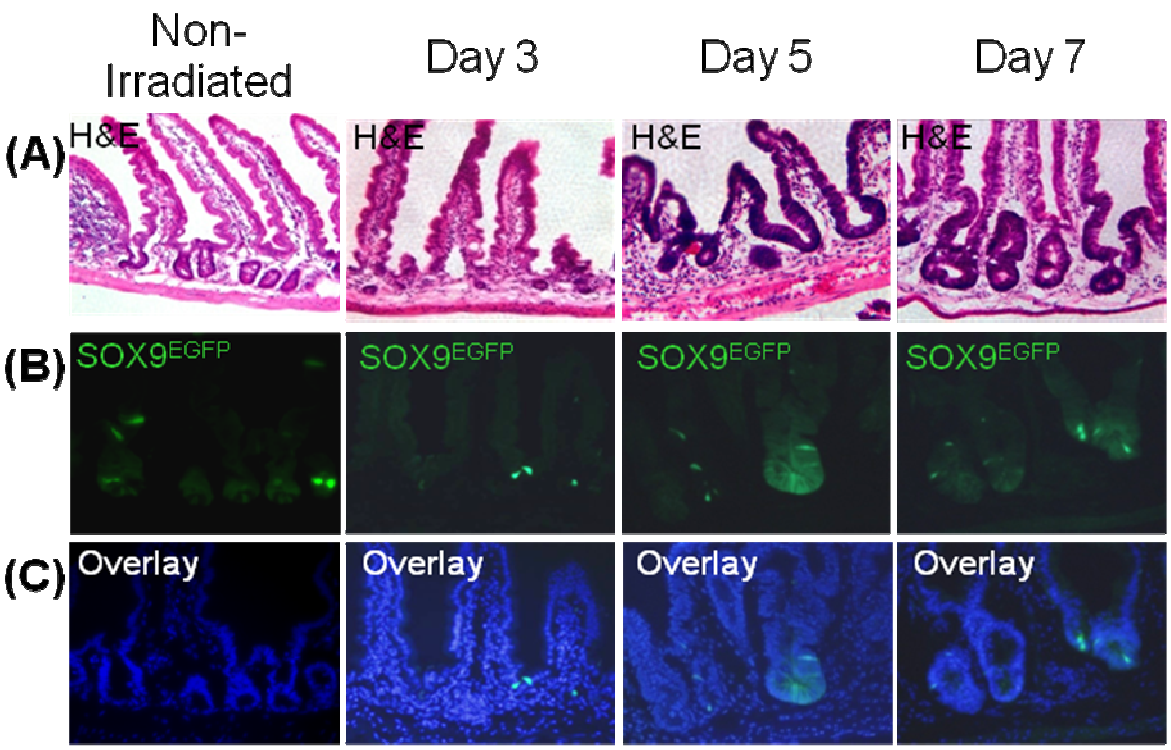

Figure 14: Sox9^{EGFPLO} cells are lost at day 3 and then show vast expansion in hyper-regenerative crypts at days 5 and 7 after irradiation. (A) H&E staining of areas representative of the immunofluorescence staining in B and C. **(B)** Distribution of Sox9^{EGFPHI} and Sox9^{EGFPLO} cells after irradiation. **(C)** Overlay of Sox9^{EGFP} and nuclear stain in blue.

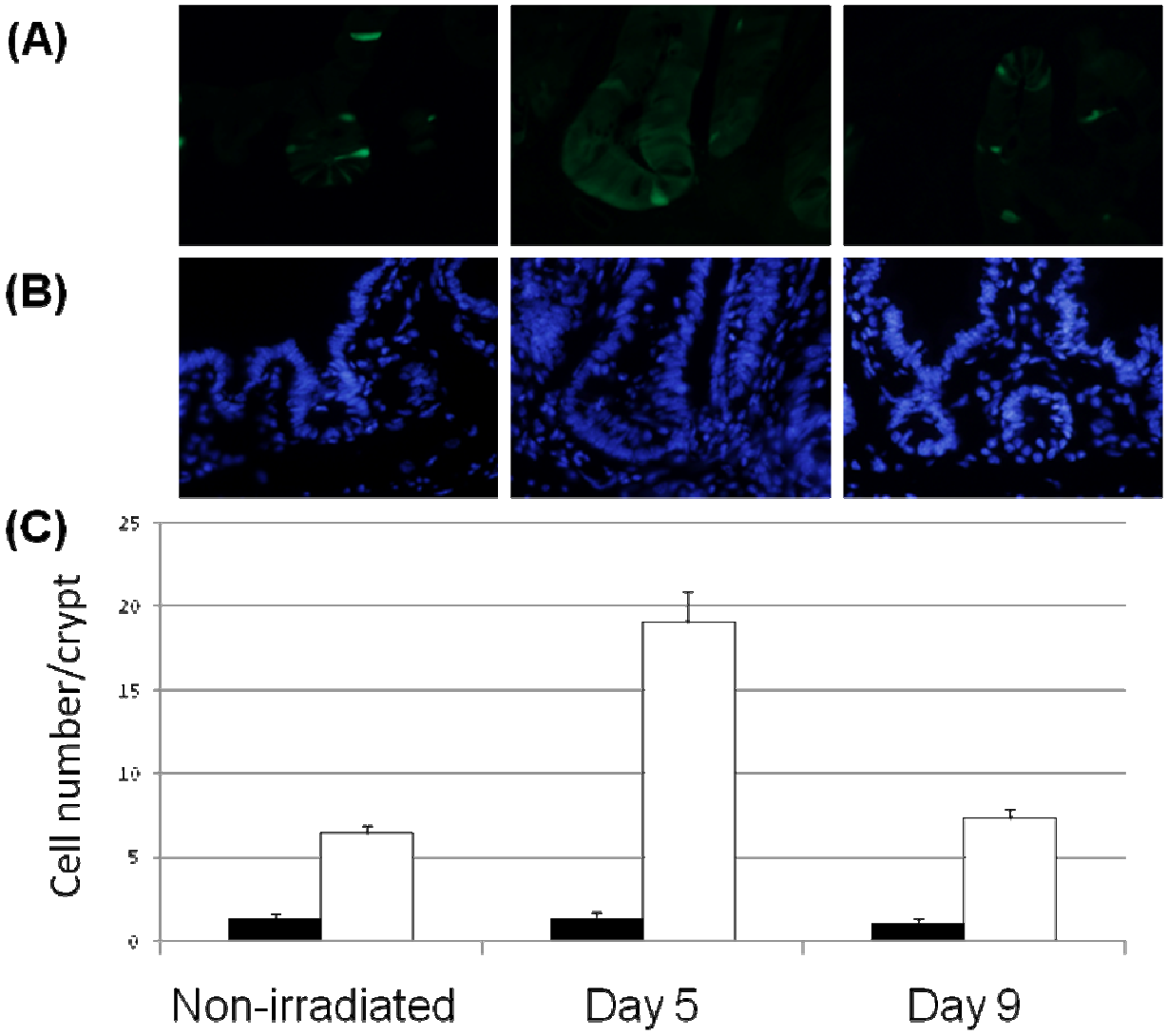

Figure 15: There is no change in the number of Sox9^{EGFPHI} cells after irradiation, while Sox9^{EGFPLO} cells increase almost 3 fold. Quantification of Sox9^{EGFPHI} (▬) and Sox9^{EGFPLO} cells (▭). (A) Sox9^{EGFP}expression. **(B)** Corresponding nuclear staing. **(C)** Sox9^{EGFP} cells were counted in 15 crypts from 1 animal at each time point. There is no change in the number of Sox9^{EGFPHI} cells at any time point, while Sox9^{EGFPLO} cells showed a 2.93 fold change (6.47±0.413 vs. 19±1.919) in hyper-regenerative crypts at day 5 after irradiation. The standard error of the mean is shown.

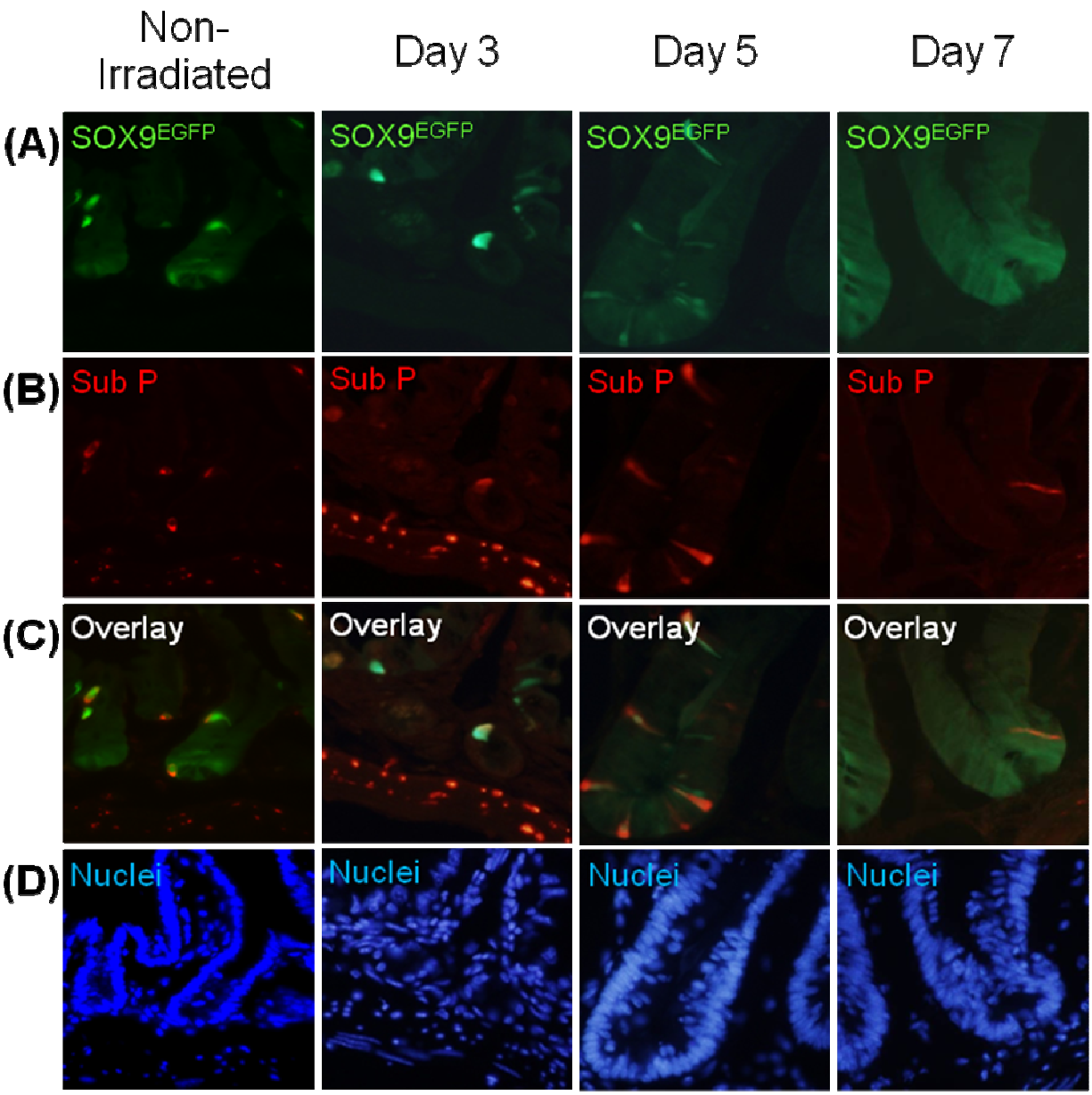

Figure 16: Sox9^{EGFPHI} cells colocalize with most Substance P expressing cells after irradiation. (A) Distribution of Sox9^{EGFPHI} and Sox9^{EGFPLO} cells after irradiation. **(B)** Immunostaining for Substance P (Sub P) in red. **(C)** Overlay of Sox9^{EGFP} and Substance P show colocalization of almost all Sox9^{EGFPHI} cells and Substance P. **(D)** Nuclear staining in blue corresponding to the pictures above.

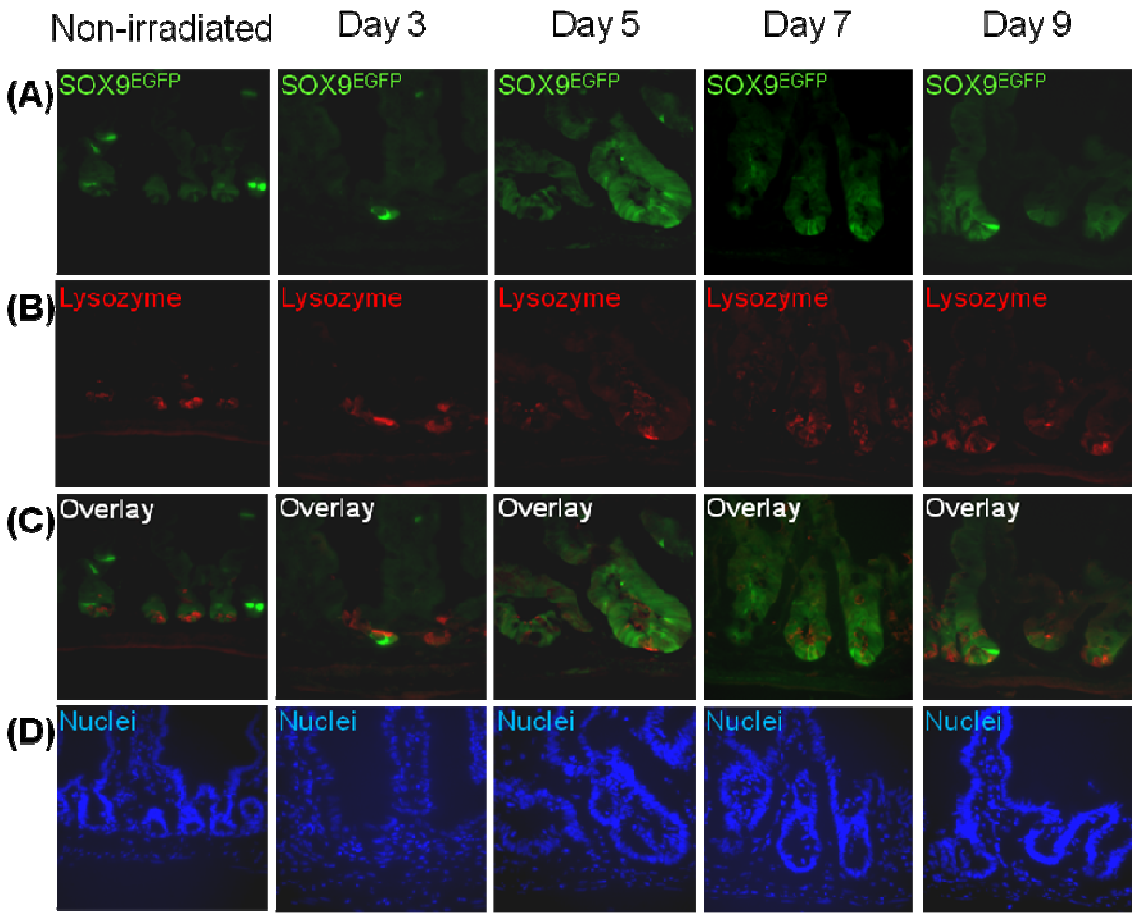

Figure 17: Lysozyme positive Paneth cells did not colocalize with Sox9^{EGFP} cells and did not show an increase at any time point after irradiation. (A) Sox9^{EGFP} shows a loss, followed by a dramatic increase in Sox9^{EGFPLO} cells with no change in Sox9^{EGFPHI} cells. **(B)** Lysozyme staining becomes blurred at day 3 and returns to a granular state at later time points. There does not appear to be an increase in Lysozyme positive cells an any time point. **(C)** Overlay of Sox9^{EGFP} and Lysozyme immunofluorescent staining showing no colocalization. **(D)** Nuclear staining in blue corresponding to the pictures above.

Chapter 4
Discussion

Whole body irradiation provides a useful experimental model, but has the potential disadvantage that a majority of WT animals die between 5 and 7 days after irradiation precluding analyses of complete crypt and villus regeneration (Qui 2008)(Potten, 2004). With this in mind, we adapted an abdominal irradiation model for our studies with the goal of improve animal survival beyond 5 – 7 days. In addition, abdominal irradiation may better mimic radiation-induced damage that occurs clinically due to regional radiation for abdominal malignancy (Kountouras, Zavos 2008). Our study using abdominal irradiation revealed that a majority of animals survived up to 7 – 9 days and began to gain or maintain weight. This suggests that the model will prove valuable for evaluating later time points in future studies. This model was then used to evaluate the expression pattern of the putative IESC marker, Sox9.

Irradiation has been widely used as a model to study crypt loss and regeneration (Potter 2004, Qui, Carson-Walter 2008). Extensive studies by Potten and colleagues have used different doses of whole body γ-irradiation to assess susceptibility of small or large bowel crypts to radiation-induced apoptosis. These analyses indicate that small intestinal crypts showed higher levels of early apoptosis at 4 – 6 hours after irradiation (the time of peak apoptosis response) compared with colon (Potten 2004). Radiation models have also been used to study crypt regeneration after radiation and most

studies have focused on days 3 through 5 after irradiation when colonies of proliferating cells or expanded crypts with proliferating cells are believed to reflect clonal expansion of intestinal stem cells surviving the injury (George 2009, Qiu 2008). However, relatively few published studies have evaluated crypt loss and regeneration after abdominal radiation along the entire length of small and large intestine in the same animals after irradiation (Freeman 2001). Our studies revealed clear regional differences in crypt loss after abdominal radiation. In the small intestine, the duodenum was most resistant to radiation-induced crypt loss with crypts remaining at all times studied, but regenerative responses still occurring by days 7 and 9. Jejunum and ileum exhibited complete crypt loss by days 3 and 5 with ileum showing significantly greater damage. The differential response to irradiation defined here by increasing injury from the proximal to the distal end of the small intestine may be reflective of differences in stem cell properties within each region. In the duodenum, there may be more IESC, these IESC may be less sensitive or have greater regenerative capacity in response to irradiation. In this regard it is noteworthy that one recently defined stem cell marker Bmi1 appears to be selectively expressed in proximal small intestine suggesting differences in stem cell populations throughout the intestine (Sangiorgi & Capecchi, 2008). Future studies to better understand the mechanisms that allow duodenal stem cells to survive and regenerate will be relevant to strategies that may increase regeneration in other areas of the intestine.

Consistent with prior findings by Potten that colon crypt cells show lower rates of irradiation induced apoptosis than the small intestine, our findings suggest that the colon was more resistant to crypt loss after 14Gy abdominal body irradiation than small

intestine. Neither proximal nor distal colon showed complete crypt loss at days 3 and 5. Furthermore, it has been observed that germ-free mice are less susceptible to radiation induced crypt damage (Crawford & Gordon, 2005). Despite this, by day 7 there was a marked increase in regenerating crypts, occurring with the appearance of inflammatory infiltrates. While more needs to be done to verify inflammation, such as staining for immune cells, this observation may reflect that damage in the colon after irradiation may lead to barrier defects that expose the underlying lamina propria to high levels of luminal microbiota that initiate an inflammatory response. This inflammatory response may be aiding regeneration after irradiation. We also speculate that the greater damage to the ileum compared to more proximal regions of the small intestine could also reflective of a difference in the inflammatory response and microbiota. Comparisons of crypt loss and regeneration across the small intestine and colon may be useful in understanding the role of inflammation during regeneration after irradiation in a setting of different degrees of damage-induced inflammation.

Biomarkers of IESC in different regions of the intestine would allow for better understanding of their responses to radiation. Based on recent evidence that Sox9 marks stem cells, our studies analyzed whether Sox9 marked regenerating crypts after radiation (Formeister et al., 2009). Co-localization of Sox9 and Ki67 immunostaining suggests that Sox9 does mark a subset of proliferating cells in jejunal microcolonies and colonic crypts at day 3 after radiation and marks even more cells in hyper-regenerating crypts later after radiation. This provides strong evidence that Sox9 is a biomarker for regenerating crypt stem or progenitors after radiation, as well as in normal small intestine.

The expression pattern and molecular properties of Sox9 positive cells was further evaluated using a $Sox9^{EGFP}$ reporter and it has been reported that $Sox9^{EGFPLO}$ cells are crypt base columnar (CBC) with stem cell like properties during a normal physiological state (Formeister et al., 2009). In this study we used a model of high dose irradiation to test if $Sox9^{EGFP}$ expression is useful for identifying IESC after injury. Results show that $Sox9^{EGFPLO}$ cells appear to be eliminated at day 3 after high dose irradiation when clonogenic IESC are present. The loss or reduction of $Sox9^{EGFPLO}$ cells, that are hypothesized to be IESC, emphasized the dynamic nature of IESC after injury and the regenerative process.

One interesting observation was that $Sox9^{EGFPHI}$ cells are still visible at day 3 after high dose irradiation, many of which colocalize with Substance P. Further characterization of these cells with other markers such as Neuorgenin 3 is needed, but it remains a possibility that these $Sox9^{EGFPHI}$ cells revert back to a stem cell like phenotype after injury, a phenomenon that has been identified in other tissues (Harrisingh et al., 2004; Zhang et al., 2009). In this scenario, the proliferating cells undergoing mitosis that are more susceptible to mutation during injury would undergo apoptosis, while a less susceptible quiescent progenitor or differentiated cell would avoid mutation and revert back to a stem cell after injury. This dedifferentiation of a $Sox9^{EGFPHI}$ enteroendocrine cell into a stem cell could represent a mechanism by which the small intestine avoids proliferation of cells with DNA damage or mutation and could explain the absence of $Sox9^{EGFPLO}$ cells. However, at this point more needs to be done to assess if $Sox9^{EGFPHI}$ cells after irradiation do revert to proliferative cells.

It is also possible that upon injury, Substance P expressing Sox9^{EGFPHI} cells enhance the survival of surrounding quiescent IESC that are not initially identified by Sox9^{EGFP} expression and have an ability to protect their original genome (Potten, Owen, & Booth, 2002). The close proximity of quiescent stem cells and Sox9^{EGFPHI} cells, both located in the upper stem cell zone, makes it plausible that there may be interactions between these cells. However, the location of quiescent IESC at position 4 above the base of the crypt is the cellular site of greatest frequency of apoptosis after irradiation (Wilkins et al., 2002). Therefore, quiescent IESC may not be the best candidate for regenerative IESC. In this case, Sox9^{EGFPHI} cells may influence surrounding cells to adapt a stem cell-like phenotype. There is evidence that Substance P increases regeneration after irradiation (Kang, Kim, Yi, & Son, 2009). The release of Substance P from Sox9^{EGFPHI} cells could conceivably provide a paracrine mechanism driving the increase in proliferation and regeneration of adjacent IESC. At present this possibility is speculative, but could be tested by Substance P neutralization or administration. The stimulation by Substance P of surrounding cells could lead them to a phenotype more like CBC that could then be identified as Sox9^{EGFPLO} cells at later time points after irradiation. This would account for the vast increase in Sox9^{EGFPLO} cells in hyper-regenerative crypts at later time points after irradiation.

The increase in Sox9^{EGFPLO} cells in hyper-regenerative crypts after irradiation is not accompanied by an increase in Paneth cells, which have been seen to decrease after irradiation (Brennan, Carr, Seed, & McCullough, 1998). The increase in Sox9^{EGFPLO} cells does occur in conjunction with an increase in proliferation in hyper-regenerative crypts suggesting that these Sox9^{EGFPLO} cells may be acting as progenitor

or stem cells. An interaction between Sox9^{EGFPHI} and Sox9^{EGFPLO} cells is supported by the observation that some hyper-regenerative crypts marked with an extensive number of Sox9^{EGFPLO} cells also have Sox9^{EGFPHI} cells often times at almost regular intervals between the Sox9^{EGFPLO} cells. This interaction may be unique to regeneration and the presence of Sox9^{EGFPHI} cells in the upper stem cell region of only some crypts during a normal physiological state could be a protective mechanism for situations when an increase in regeneration is needed, such as after injury. Further understanding of the unique expression pattern and molecular characteristic of Sox9^{EGFP} cells after injury could help us to define the IESC phenotype and niche driving the regenerative process.

This study would be greatly enhanced with further evaluation of current samples and more animals using confocal microscopy. In this regard, I recently completed additional experiments to increase the sample size to at least four animals per time point at 3 – 9 days after irradiation. Ongoing analyses of these samples and detailed characterization of EdU colocalization with IESC biomarkers or markers of differentiated cells will provide important information to optimally design future growth factor interventions. We also have begun fluorescent-activated cell sorting (FACS) analysis to quantitatively assess the relative proportions of Sox9^{EGFPHI} and Sox9^{EGFPLO} cells at different times after irradiation. This could confirm the absence of Sox9^{EGFPLO} cells at day 3 after irradiation as the regenerative process may only require a few surviving stem cells and the identification of Sox9^{EGFPLO} cells at day 3 after irradiation by histological analysis alone may not be sufficient. Quantification through FACS analysis may also confirm of the expansion of Sox9^{EGFPLO} during regeneration.

FACS sorting can also be used to isolate $Sox9^{EGFP}$ cells for microarray analysis. Comparing the molecular phenotype of $Sox9^{EGFP}$ cells from non-irradiated mice with cells from mice at different time points after irradiated could identify genes that are important in stimulating regeneration. These genes will be relevant to developing therapies to promote IESC regeneration in patients exposed to irradiation. It would also determine the molecular differences between steady-state IESC and IESC post-irradiation. Understanding these differences is important, because as this study exemplifies there are major dramatic differences in Sox9 cells during steady-state regeneration and during the regenerative process stimulated by injury.

$Sox9^{EGFP}$ cells isolated by FACS can also be used for *in vitro* studies. One *in vitro* study that would test the dedifferentiation of $Sox9^{EGFPHI}$ cells into IESC could be done by isolating $Sox9^{EGFPHI}$ cells from normal intestinal tissue, exposing them to high-dose irradiation and maintaining them in culture to determine if they dedifferentiate. $Sox9^{EGFPLO}$ cells could also be isolated and treated with Substance P to determine if Substance P increases proliferation.

This study focused on proliferation during the regenerative process after high dose irradiation, but this abdominal irradiation model in conjunction with stem cell markers can also be used to determine the radiosensitivity of different IESC populations at different doses of irradiation. The highest rate of apoptosis occurs around 4 hours at position +4 in the USZ after low dose irradiation, but there is apoptosis at all positions (Potten & Grant, 1998) (Potten, 1992). Recent work demonstrated that maximum apoptosis in the USZ is reached at 1Gy, while maximum apoptosis of CBC cells in LSZ

is reached at 10Gy (Barker, van Es, Kuipers, Kujala, van den Born, Cozijnsen, Haegebarth, Korving, Begthel, Peters, & Clevers, 2007b). Therefore the expression pattern of $Sox9^{EGFP}$ should be evaluated at 4 hours after irradiation at both high and low doses of irradiation to determine the relative radiosensitivity of $Sox9^{EGFPHI}$ cells in the USZ and $Sox9^{EGFPLO}$ cells in the LSZ.

This irradiation model can also be used for preclinical testing of potential therapies for patients undergoing abdominal radiation therapy. It is estimated that 60-80% of cancer patients that undergo radiation therapy show signs of acute bowel toxicity which include diarrhea, abdominal pain and nausea. Delayed bowel toxicity is characterized by malabsorption and bowel dysmotility (Hauer-Jensen, Wang, Boerma, Fu, & Denham, 2007). Multiple growth factors have been investigated for their therapeutical properties, but this has been based on their ability to increase the number of microcolonies at early time points after in high-dose irradiation (Potten et al., 1995). The use of this abdominal irradiation model with $Sox9^{EGFP}$ reporter mice, other reporter mice or lineage tracing models can directly test the expansion and differentiation of stem cells throughout the regenerative process.

Insulin-like growth factor I (IGF-I) has potential as a therapy for abdominal irradiation patients. IGF-I transgenic mice have enhanced intestinal growth and show increase proliferation in crypts (Ohneda, Ulshen, Fuller, D'Ercole, & Lund, 1997). It has also been shown that IGF-I decreases apoptosis in crypts at 4 hours after 5Gy of irradiation, having the greatest affect in the USZ (Wilkins et al., 2002). Furthermore, IGF-I can suppress PUMA, a p53 dependent protein, that has been seen to increase the

radiosensitivity of cells in the IESC zone after irradiation (Han et al., 2001; Qiu et al., 2008). The model of abdominal irradiation developed in this study can be used to determine if IGF-I treatment protects $Sox9^{EGFP}$ cells from apoptosis. It will be interesting to diescover if IGF-I protects $Sox9^{EGFPHI}$ cells at low doses of irradiation, while protecting $Sox9^{EGFPLO}$ cells at high doses of irradiation, and to observe any difference in the regenerative process.

The abdominal irradiation model developed in this study provides a useful model for studying IESC and regeneration. This model resulted in increased survival compared to previously models used in other studies. This will allow for better analysis of regeneration after irradiation and the role of IESC during this process. It was observed in this study that Sox9 marked proliferating cells in microcolonies and regenerative areas. It was also seen that $Sox9^{EGFPLO}$ cells, which could not be identified with immunostaining with differentiated cell markers, were greatly expanded throughout regenerative crypts. Together this suggests that Sox9 is a useful marker of IESC after irradiation. Future studies using this model can test other IESC markers, including LGR5 and Bmi1, to understand how they react to irradiation. This could give us insight into whether there are different IESC populations that have varying responses to injury. Finally, future studies can test therapies that may have the potential to help cancer patients undergoing radiation therapy and define the effects of growth factors on cell phenotype. Evidence suggests that IGF-I could be an effective therapy for patients undergoing radiation therapy. Our laboratory plans to assess IGF-I in the $Sox9^{EGFP}$ irradiation model and to cross $Sox9^{EGFP}$ and another stem cell reporter mouse, Lgr5-LacZ mice, with the IGF-I transgenic mice to further define the role of IGF-I in stem cell

proliferation, expansion or regeneration in normal or irradiated intestine. This radiation model will allow us to gain greater knowledge of IESC and therapies that can increase their survival and regeneration to help people exposed to irradiation.

Appendix 1

Biochomoendoscopy and Ileo-cecal resection of CONV-IL-10 null mice

The focus of my independent research project on the irradiation model is presented in the main thesis. I also participated in two other studies aimed at improved visualization of gastrointestinal tumors using molecular probes and development of an ileo-cecal resection model in IL-10 null mice, as a model to analyze stem cells during post-surgical adaptive growth of small intestine in a setting of inflammation. Co-authorship on two publications resulted from my participation in these projects as listed below:

Zhang H, Morgan D, Cecil G, Burkholder A, Ramocki N, Scull B, Lund PK. Biochromoendoscopy: molecular imaging with capsule endoscopy for detection of polypoid lesions in the GI tract. Gastrointestinal Endoscopy 2008; 68(3):520-7. PMID: 18499106.

Rigby RJ, Hunt MR, Scull BP, Helmrath MA, Lund PK. A new animal model of post-surgical inflammatory bowel disease and fibrosis: the effect of commensal microflora. Gut 2009. PMID: 19398439. In Press.

The abstract from these publications are provided as appendix material.

Appendix 2

Biochromoendoscopy: molecular imaging with capsule endoscopy for detection of polypoid lesions in the GI tract.

BACKGROUND: Current capsule endoscopy (CE) provides minimally invasive technology for GI imaging but has limited ability to diescriminate different types of polyps. Near infrared fluorescent (NIRF) probes activated by biomarkers upregulated in adenomas (eg, cathepsin B) are potentially powerful tools to distinguish premalignant or malignant lesions from benign or inflammatory lesions. OBJECTIVES: To examine whether CE can be integrated with NIRF probes to detect adenomas and whether cathepsin B-activated NIRF probes are activated by benign or inflammatory lesions. DESIGN: Mouse models of adenomas, hyperplactic/lymphoid polyps, and acute or chronic intestinal inflammation were injected intravenously with a cathepsin B-activated probe (Prosense 680). Dissected intestine was imaged with CE under white or NIRF light. For NIRF excitation (680 nm), dichroic and emission (700 nm) filters were combined with CE when images were recorded. Prosense 680 samples with or without protease were used as positive and negative controls. CE-based imaging data were verified by using and independent imaging system (Xenogen IVIS system). MAIN OUTCOME MEASUREMENTS: Proof of principal that CE integrated with NIRF probes can detect and diescriminate adenomas from other lesions. RESULTS: CE-based NIRF imaging with Prosense 680 readily visualized adenomas, including in the colitis model. NIRF signals of different intensities were detected. Prosense 680 was not activated by benign or inflammatory lesions. LIMITATION: Optical filters external to the capsule were

used. CONCLUSIONS: We demonstrate proof of the principle that biochromoendoscopy-CE combined with molecular probes--provides a novel approach that differentiates adenomas from benign polyps and inflammatory lesions.

Appendix 3

A new animal model of post-surgical inflammatory bowel disease and fibrosis: the effect of commensal microflora.

OBJECTIVE: Ileo-cecal resection (ICR) is common in Crohn's disease (CD). Inflammation and fibrosis frequently recur at the site of anastomosis or in the small intestine (SI). No animal models of post-surgical inflammation and fibrosis exist. We developed a model of ICR in IL-10 null and wild-type (WT) mice to test the hypothesis that that ICR promotes post-surgical inflammation and fibrosis in SI or anastomosis of genetically susceptible IL-10 null, but not WT or germ free (GF)-IL-10 null mice. DESIGN: GF-IL-10 null mice were conventionalized (CONV) and 3 weeks later randomized to ICR, transection (T) or no treatment (NoTx). Age-matched conventionally raised (CONV) WT and GF-IL-10 null mice received ICR, T or NoTx. Animals were killed 28 days later. MAIN OUTCOME MEASURES: Histological scoring, real-time PCR for TNFalpha and collagen, and immunostaining for CD3+ T cells, assessed inflammation and fibrosis. RESULTS: After ICR, CONV-IL-10 null, but not CONV-WT mice, developed significant inflammation and fibrosis in SI and inflammation in anastomosis compared to NoTx or T controls. Fibrosis occurred in anastomosis of both CONV-IL-10 null and CONV-WT following ICR. GF-IL-10 null mice developed little or no inflammation or fibrosis in SI or anastomosis after ICR. CONCLUSIONS: ICR in CONV-IL-10 null mice provides a new animal model of post-surgical inflammation and fibrosis in SI and anastomosis. Absence of inflammation and fibrosis in SI of CONV-WT and

GF-IL-10 null following ICR indicates that post-surgical small bowel disease occurs only in genetically susceptible IL-10 null mice and is bacteria dependent.

References

Arsenijevic, Y. (2005). Future perspectives: From stem cells and IGF biology to the clinic. *Advances in Experimental Medicine and Biology, 567*, 385-412.

Barker, N., van Es, J. H., Kuipers, J., Kujala, P., van den Born, M., Cozijnsen, M., et al. (2007a). Identification of stem cells in small intestine and colon by marker gene Lgr5. *Nature, 449*(7165), 1003-1007.

Barker, N., van Es, J. H., Kuipers, J., Kujala, P., van den Born, M., Cozijnsen, M., et al. (2007b). Identification of stem cells in small intestine and colon by marker gene Lgr5. *Nature, 449*(7165), 1003-1007.

Batlle, E., Henderson, J. T., Beghtel, H., van den Born, M. M., Sancho, E., Huls, G., et al. (2002). Beta-catenin and TCF mediate cell positioning in the intestinal epithelium by controlling the expression of EphB/ephrinB. *Cell, 111*(2), 251-263.

Beaulieu, J. F. (1992). Differential expression of the VLA family of integrins along the crypt-villus axis in the human small intestine. *Journal of Cell Science, 102 (Pt 3)*(Pt 3), 427-436.

Bjerknes, M., & Cheng, H. (2002). Multipotential stem cells in adult mouse gastric epithelium. *American Journal of Physiology.Gastrointestinal and Liver Physiology, 283*(3), G767-77.

Bjerknes, M., & Cheng, H. (2006). Intestinal epithelial stem cells and progenitors. *Methods in Enzymology, 419*, 337-383.

Booth, C., Booth, D., Williamson, S., Demchyshyn, L. L., & Potten, C. S. (2004). Teduglutide ([Gly2]GLP-2) protects small intestinal stem cells from radiation damage. *Cell Proliferation, 37*(6), 385-400.

Brennan, P. C., Carr, K. E., Seed, T., & McCullough, J. S. (1998). Acute and protracted radiation effects on small intestinal morphological parameters. *International Journal of Radiation Biology, 73*(6), 691-698.

Cai, W. B., Roberts, S. A., Bowley, E., Hendry, J. H., & Potten, C. S. (1997). Differential survival of murine small and large intestinal crypts following ionizing radiation. *International Journal of Radiation Biology, 71*(2), 145-155.

Cheng, H., & Leblond, C. P. (1974). Origin, differentiation and renewal of the four main epithelial cell types in the mouse small intestine. V. unitarian theory of the origin of the four epithelial cell types. *The American Journal of Anatomy, 141*(4), 537-561.

Crawford, P. A., & Gordon, J. I. (2005). Microbial regulation of intestinal radiosensitivity. *Proceedings of the National Academy of Sciences of the United States of America, 102*(37), 13254-13259.

de Santa Barbara, P., van den Brink, G. R., & Roberts, D. J. (2003). Development and differentiation of the intestinal epithelium. *Cellular and Molecular Life Sciences : CMLS, 60*(7), 1322-1332.

Dube, P. E., Forse, C. L., Bahrami, J., & Brubaker, P. L. (2006). The essential role of insulin-like growth factor-1 in the intestinal tropic effects of glucagon-like peptide-2 in mice. *Gastroenterology, 131*(2), 589-605.

Formeister, E. J., Sionas, A. L., Lorance, D. K., Barkley, C. L., Lee, G. H., & Magness, S. T. (2009). Distinct SOX9 levels differentially mark Stem/Progenitor populations and enteroendocrine cells of the small intestine epithelium. *American Journal of Physiology.Gastrointestinal and Liver Physiology,*

Giannakis, M., Stappenbeck, T. S., Mills, J. C., Leip, D. G., Lovett, M., Clifton, S. W., et al. (2006). Molecular properties of adult mouse gastric and intestinal epithelial progenitors in their niches. *The Journal of Biological Chemistry, 281*(16), 11292-11300.

Gibson, P. R. (2004). Apoptosis or necrosis--colonic epithelial cell survival. *Novartis Foundation Symposium, 263*, 133-45; diescussion 145-50, 211-8.

Gong, S., Zheng, C., Doughty, M. L., Losos, K., Didkovsky, N., Schambra, U. B., et al. (2003). A gene expression atlas of the central nervous system based on bacterial artificial chromosomes. *Nature, 425*(6961), 917-925.

Han, J., Flemington, C., Houghton, A. B., Gu, Z., Zambetti, G. P., Lutz, R. J., et al. (2001). Expression of bbc3, a pro-apoptotic BH3-only gene, is regulated by diverse cell death and survival signals. *Proceedings of the National Academy of Sciences of the United States of America, 98*(20), 11318-11323.

Harrisingh, M. C., Perez-Nadales, E., Parkinson, D. B., Malcolm, D. S., Mudge, A. W., & Lloyd, A. C. (2004). The Ras/Raf/ERK signalling pathway drives schwann cell dedifferentiation. *The EMBO Journal, 23*(15), 3061-3071.

Hauer-Jensen, M., Wang, J., Boerma, M., Fu, Q., & Denham, J. W. (2007). Radiation damage to the gastrointestinal tract: Mechanisms, diagnosis, and management. *Current Opinion in Supportive and Palliative Care, 1*(1), 23-29.

He, X. C., Yin, T., Grindley, J. C., Tian, Q., Sato, T., Tao, W. A., et al. (2007). PTEN-deficient intestinal stem cells initiate intestinal polyposis. *Nature Genetics, 39*(2), 189-198.

He, X. C., Zhang, J., Tong, W. G., Tawfik, O., Ross, J., Scoville, D. H., et al. (2004). BMP signaling inhibits intestinal stem cell self-renewal through suppression of wnt-beta-catenin signaling. *Nature Genetics, 36*(10), 1117-1121.

Hendry, J. H., Roberts, S. A., & Potten, C. S. (1992). The clonogen content of murine intestinal crypts: Dependence on radiation dose used in its determination. *Radiation Research, 132*(1), 115-119.

Ishizuka, S., Martin, K., Booth, C., Potten, C. S., de Murcia, G., Burkle, A., et al. (2003). Poly(ADP-ribose) polymerase-1 is a survival factor for radiation-exposed intestinal epithelial stem cells in vivo. *Nucleic Acids Research, 31*(21), 6198-6205.

Kang, M. H., Kim, D. Y., Yi, J. Y., & Son, Y. (2009). Substance P accelerates intestinal tissue regeneration after gamma-irradiation-induced damage. *Wound Repair and Regeneration : Official Publication of the Wound Healing Society [and] the European Tissue Repair Society, 17*(2), 216-223.

Khan, W. B., Shui, C., Ning, S., & Knox, S. J. (1997). Enhancement of murine intestinal stem cell survival after irradiation by keratinocyte growth factor. *Radiation Research, 148*(3), 248-253.

Krysiak, R., Gdula-Dymek, A., Bednarska-Czerwinska, A., & Okopien, B. (2007). Growth hormone therapy in children and adults. *Pharmacological Reports : PR, 59*(5), 500-516.

Marshman, E., Ottewell, P. D., Potten, C. S., & Watson, A. J. (2001). Caspase activation during spontaneous and radiation-induced apoptosis in the murine intestine. *The Journal of Pathology, 195*(3), 285-292.

Morante, J., Vallejo-Cremades, M. T., Gomez-Garcia, L., Vazquez, I., Gomez-de-Segura, I. A., Sanchez, M., et al. (2003). Differential action of growth hormone in irradiated tumoral and nontumoral intestinal tissue. *Digestive Diseases and Sciences, 48*(11), 2159-2166.

Ohneda, K., Ulshen, M. H., Fuller, C. R., D'Ercole, A. J., & Lund, P. K. (1997). Enhanced growth of small bowel in transgenic mice expressing human insulin-like growth factor I. *Gastroenterology, 112*(2), 444-454.

Potten, C. S. (1992). The significance of spontaneous and induced apoptosis in the gastrointestinal tract of mice. *Cancer Metastasis Reviews, 11*(2), 179-195.

Potten, C. S. (2004). Radiation, the ideal cytotoxic agent for studying the cell biology of tissues such as the small intestine. *Radiation Research, 161*(2), 123-136.

Potten, C. S., & Booth, C. (1997). The role of radiation-induced and spontaneous apoptosis in the homeostasis of the gastrointestinal epithelium: A brief review. *Comparative Biochemistry and Physiology.Part B, Biochemistry & Molecular Biology, 118*(3), 473-478.

Potten, C. S., Booth, C., Tudor, G. L., Booth, D., Brady, G., Hurley, P., et al. (2003). Identification of a putative intestinal stem cell and early lineage marker; musashi-1. *Differentiation; Research in Biological Diversity, 71*(1), 28-41.

Potten, C. S., & Grant, H. K. (1998). The relationship between ionizing radiation-induced apoptosis and stem cells in the small and large intestine. *British Journal of Cancer, 78*(8), 993-1003.

Potten, C. S., & Loeffler, M. (1990). Stem cells: Attributes, cycles, spirals, pitfalls and uncertainties. lessons for and from the crypt. *Development (Cambridge, England), 110*(4), 1001-1020.

Potten, C. S., Merritt, A., Hickman, J., Hall, P., & Faranda, A. (1994). Characterization of radiation-induced apoptosis in the small intestine and its biological implications. *International Journal of Radiation Biology, 65*(1), 71-78.

Potten, C. S., Owen, G., & Booth, D. (2002). Intestinal stem cells protect their genome by selective segregation of template DNA strands. *Journal of Cell Science, 115*(Pt 11), 2381-2388.

Potten, C. S., Owen, G., Hewitt, D., Chadwick, C. A., Hendry, H., Lord, B. I., et al. (1995). Stimulation and inhibition of proliferation in the small intestinal crypts of the mouse after in vivo administration of growth factors. *Gut, 36*(6), 864-873.

Qiu, W., Carson-Walter, E. B., Liu, H., Epperly, M., Greenberger, J. S., Zambetti, G. P., et al. (2008). PUMA regulates intestinal progenitor cell radiosensitivity and gastrointestinal syndrome. *Cell Stem Cell, 2*(6), 576-583.

Radford, I. R., & Lobachevsky, P. N. (2006). An enteroendocrine cell-based model for a quiescent intestinal stem cell niche. *Cell Proliferation, 39*(5), 403-414.

Ramocki, N. M., Wilkins, H. R., Magness, S. T., Simmons, J. G., Scull, B. P., Lee, G. H., et al. (2008). Insulin receptor substrate-1 deficiency promotes apoptosis in the putative intestinal crypt stem cell region, limits apcmin/+ tumors, and regulates Sox9. *Endocrinology, 149*(1), 261-267.

Rindi, G., Leiter, A. B., Kopin, A. S., Bordi, C., & Solcia, E. (2004). The "normal" endocrine cell of the gut: Changing concepts and new evidences. *Annals of the New York Academy of Sciences, 1014*, 1-12.

Sancho, E., Batlle, E., & Clevers, H. (2004). Signaling pathways in intestinal development and cancer. *Annual Review of Cell and Developmental Biology, 20*, 695-723.

Sangiorgi, E., & Capecchi, M. R. (2008). Bmi1 is expressed in vivo in intestinal stem cells. *Nature Genetics, 40*(7), 915-920.

Sato, T., Vries, R. G., Snippert, H. J., van de Wetering, M., Barker, N., Stange, D. E., et al. (2009). Single Lgr5 stem cells build crypt-villus structures in vitro without a mesenchymal niche. *Nature, 459*(7244), 262-265.

Schuller, B. W., Rogers, A. B., Cormier, K. S., Riley, K. J., Binns, P. J., Julius, R., et al. (2007). No significant endothelial apoptosis in the radiation-induced gastrointestinal syndrome. *International Journal of Radiation Oncology, Biology, Physics, 68*(1), 205-210.

Wang, J., Boerma, M., Fu, Q., & Hauer-Jensen, M. (2007). Significance of endothelial dysfunction in the pathogenesis of early and delayed radiation enteropathy. *World Journal of Gastroenterology : WJG, 13*(22), 3047-3055.

Wilkins, H. R., Ohneda, K., Keku, T. O., D'Ercole, A. J., Fuller, C. R., Williams, K. L., et al. (2002). Reduction of spontaneous and irradiation-induced apoptosis in small intestine of IGF-I transgenic mice. *American Journal of Physiology.Gastrointestinal and Liver Physiology, 283*(2), G457-64.

Winton, D. J., & Brooks, R. A. (1998). Analysis of DNA damage and repair accompanying differentiation in the intestinal crypt. *Philosophical Transactions of the Royal Society of London.Series B, Biological Sciences, 353*(1370), 895-902.

Ye, P., & D'Ercole, A. J. (2006). Insulin-like growth factor actions during development of neural stem cells and progenitors in the central nervous system. *Journal of Neuroscience Research, 83*(1), 1-6.

Zhang, C., Fu, X., Chen, P., Bao, X., Li, F., Sun, X., et al. (2009). Dedifferentiation-derived cells exhibit phenotypic and functional characteristics of epidermal stem cells. *Journal of Cellular and Molecular Medicine,*